Joint Maintenance Planning of Deteriorating Co-located Road and Water Infrastructures with Interdependencies

Hung Nguyen[a], Noha Abdel-Mottaleb[b], Shihab Uddin[b], Qiong Zhang[b], Qing Lu[b], He Zhang[c], Mingyang Li[a,*]

[a] *Department of Industrial and Management Systems Engineering, University of South Florida, 4202 E. Fowler Avenue, Tampa, FL 33620, United States*
[b] *Department of Civil and Environmental Engineering, University of South Florida, 4202 E. Fowler Avenue, Tampa, FL 33620, United States*
[c] *Department of Information Systems Decision Sciences, University of South Florida, 4202 E. Fowler Avenue, Tampa, FL 33620, United States*

Abstract

Due to co-location and spatial proximity, deteriorating water infrastructure (WI) and transportation infrastructure (TI) have complex interdependencies, including both physical dependency from road to pipe, and operational dependency from pipe to road. On one hand, traffic load is not only a dominant factor for the physical degradation of road but may also be an important contributing factor to the sudden failure of the pipe underneath the co-located road due to the extreme propagated stress. On the other hand, the water pipe breaks and repairs will also cause traffic blockage, lane closure, and repaving of road surface, which influence both road user costs and road maintenance costs. Most of the existing maintenance work mainly considered WI and TI separately but neglected their complex interdependencies. This study proposes a joint proactive maintenance planning framework for the co-located road and pipe under their degradation uncertainties by explicitly taking into account both their physical and operational dependencies. In particular, the competing failure modes of both the traffic-induced sudden failure and the corrosion-induced gradual failure are simultaneously considered for the pipe to capture the physical dependency. Road maintenance costs and road user costs in the presence of pipe maintenance disruption are also formulated for the road to capture the operational dependency. A case study is further provided to comprehensively evaluate the performance of the proposed joint maintenance planning strategy over several existing benchmark strategies and demonstrate the cost-saving benefit of the proposed work. The impacts of interdependencies on the proposed maintenance planning decisions are also thoroughly investigated.

Keywords: Co-located road and pipe, joint maintenance, cost saving, interdependent infrastructures, aging infrastructures.

*Corresponding author
Email address: mingyangli@usf.edu (Mingyang Li)

1. Introduction

Serving as the backbone of the nation's economy, a large number of deteriorating critical infrastructures, such as transportation infrastructure (TI) and water infrastructure (WI), are underperforming, structurally deficient and must be repaired or replaced. According to the Department of Transportation (DOT) 2019 report, there are 240,324 miles of highway (∼66%)in the United States (U.S.) in fair, poor, and very poor condition [1]. In addition, 43% of installed pipes in the U.S. in 2018 are in the range of 20 to 50 years old, and 28% are over 50 years old, which are consistent with a significant 27% increase in break rate from 2012 [2]. The underperformance and deficiency of roads and pipes have tremendous impacts on economic growth, social development, and public safety of modern society. Poor road conditions can contribute to the decrease of ride quality and increase of crash rate, fuel consumption and, vehicle emission exhaust, as well as transportation agencies' maintenance costs and vehicle repair and operating costs; in extreme events of natural hazards, poor road infrastructure can also impede emergency response to ensure safety and shelter for the impacted communities [3]. Meanwhile, pipe breaks and leaks will increase water loss and unmet water demand, decrease water quality, and increase maintenance and rehabilitation costs. Facing the poor conditions of infrastructures and limited federal financing or public investment for infrastructure maintenance, there is a pressing need to develop a proactive and cost-effective maintenance planning model to ensure high-quality performance and long-term reliability of existing TI and WI.

Field degradation of TI and WI are highly uncertain and stochastic due to the influence of many unknown/unobserved factors at different phases of lifecycle, including material structure and design, construction conditions, and environmental conditions. Due to co-location and spatial proximity, TI and WI are physically and operationally interdependent [4], providing additional complexity for proactive maintenance planning. From a physical degradation perspective, the traffic load from roads will not only affect the degradation of roads but may also create sudden structure failures of water mains underneath the road due to the damage from external heavy loading [5]. From an operational maintenance perspective, the pipe repairs due to water breaks will also cause lane closures, lead to traffic blockage, and significantly affect the mobility and efficiency of the roads [6]. In addition, interdependent TI and WI may offer opportunities to save maintenance and rehabilitation costs if the maintenance planning decisions from roads and pipes can be jointly determined. Instead of maintaining co-located road and pipe separately at different time periods, which often increases traffic blockage and duplicates the repaving of co-located surface, the joint maintenance of them in the same time period can potentially avoid repaving twice and reduce the number of crew members, machines, and materials used for maintenance activities. In the existing maintenance literature and practice for WI [7, 8] and TI [9–11], their maintenance decisions are determined or optimized

separately without taking into account the aforementioned interdependencies and the joint maintenance strategy. There are also several existing studies that investigated the risk assessment [12, 13], resilience analysis [12–14], and system restoration [15, 16]. These studies either focused on a single infrastructure [14] or a network of interdependent infrastructures [12, 13, 15, 16]. To investigate the impact of the interdependencies between infrastructures, [12, 15, 16] considered the topology of the network, while [13] studied the operational dependency from the building damage to traffic blockage, and [14] focused on the physical dependency between systems in the energy infrastructure. In addition, these studies mainly focused on improving the system resilience/restoration process at the post-extreme event phase, such as post-earthquake phase [12, 13, 16], or during both pre- and post-disruption periods [14, 15]. Lastly, the time duration of the above studies may range from days to months, depending on the total time needed for system recovery/restoration. There are still research needs for (i) investigating the maintenance planning for interdependent co-located infrastructures during their normal operating conditions (e.g., such as the deteriorating and co-located road and pipe in the field); (ii) accounting for multiple types of dependencies between infrastructures (e.g., physical and operational dependencies); and (iii) providing a long-term maintenance plan (over years) for system improvement.

In the existing maintenance literature for proactive maintenance planning, different maintenance approaches, such as time-based maintenance and condition-based maintenance, have been developed (and for a comprehensive review, please refer to [17] and references therein). Among them, many studies have focused on studying independent components/systems [18, 19] and there is limited work for capturing the detailed dependencies/interdependencies among different components/systems. Dekker et al. [20] categorized such dependencies/interdependencies into three categories, namely stochastic dependence [20–23], economic dependence [20, 24, 25], and structural dependence [26], and most of the existing maintenance planning models mainly focused on addressing one of these dependencies. Due to the highly complex interdependences between WI and TI, all three dependencies exist. Specifically, stochastic dependence exists when the deteriorating state of a component affects the condition state of other components. For the co-located road and pipe, the road condition and traffic-load effect will potentially influence the underneath pipe with increased risk of pipe breaks. Economic dependence exists when maintaining several components jointly instead of separately can either reduce or increase the cost. For the co-located road and pipe, joint maintaining them in the same time period may potentially reduce the overall maintenance cost by avoiding multiple times of re-paving the co-located areas. Structural dependence exists when maintaining one component initiates/influences the maintenance activities for other components. For the co-located road and pipe, repairing pipe may disrupt the service operations of the road due to lane closes or traffic blockage, and the maintenance plans of the road need to be adjusted accordingly to reduce the overall negative impacts of maintenance activities on road users. Thus, there is the need to develop a maintenance planning framework that could simultaneously

take into account all the above three dependencies.

To fill the aforementioned research gaps, this paper proposes a joint long-term maintenance planning framework for the co-located and deteriorating road and pipe under field degradation uncertainties by explicitly capturing their interdependent complexities, including both physical dependency from road to pipe as well as operational dependency from pipe to road. A stochastic degradation model for the co-located road and pipe is first established to capture field degradation uncertainties as well as integrate physical dependency captured by the finite element models. The competing failure modes of pipes, including both the corrosion-induced gradual failure mode and traffic-load-induced sudden failure mode (due to the influence of traffic load from road side), are explicitly considered in the developed degradation model. Then a joint maintenance planning model is established by taking into account the operational dependency between pipe and road under different co-located scenarios to minimize the overall cost, including both short-term maintenance costs and long-term user costs. The proposed work advances the reliability engineering literature by developing a long-term joint maintenance planning framework for interdependent and co-located road and pipe infrastructures to account for their multiple dependency structures (e.g., both physical and operational dependencies).

The remainder of this paper is organized as follows: Section 2.1 introduces the modeling of field degradation of road and pipe with physical dependency; Section 2.2 provides the formulation for the joint maintenance optimization of co-located road and pipe with operational dependency; Section 3.1 shows the real case study setup; Section 3.2 provides the performance comparison between the proposed maintenance strategy and traditional ones; Section 3.3 provides the details on the influence of road and pipe interdependencies on maintenance decisions and cost values; and Section 4 draws the conclusions.

2. Methodology

In this study, a joint maintenance decision-making framework is proposed for the co-located road and pipe by taking into account their physical and operational dependencies. Fig. 1 gives an overview of the proposed framework, which consists of four major steps. The first step is to model both the road and pipe degradation performance, in particular, finite element analysis (FEA) will be utilized to capture the physical dependency from road to pipe. The second and third steps are to formulate the joint maintenance optimization model by incorporating the operational dependency from pipe to road and then to solve the optimization model using the backward induction method. The last step is to compare the proposed work with several existing maintenance strategies as benchmarks and to further perform sensitivity analysis of the proposed work. The details of each step will be elaborated in the following subsections.

2.1. Degradation performance modeling of road and pipe with physical dependency

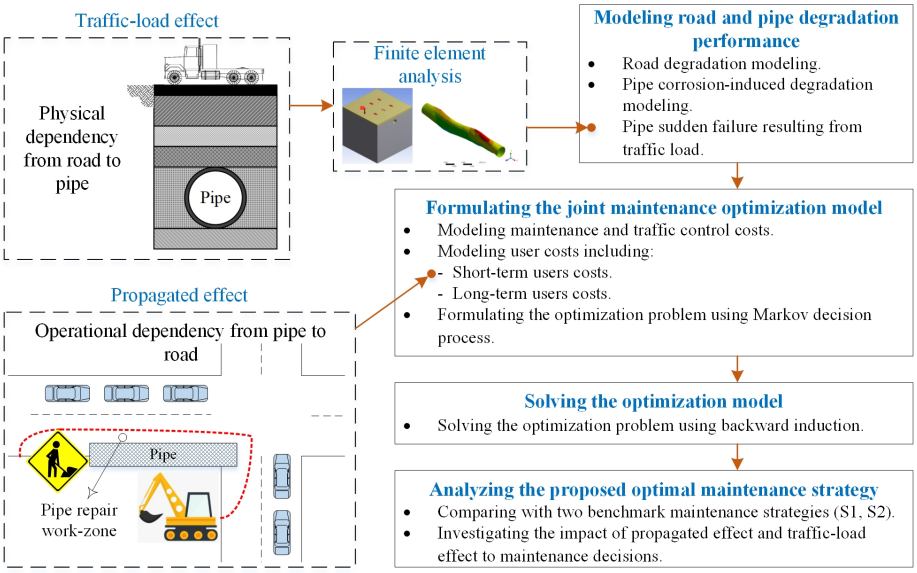

Figure 1: The overview of the proposed framework.

2.1.1. Road degradation performance modeling

The degradation performance of a deteriorating road segment is often measured by its service performance indicators. The values of these indicators are collected through the annual field inspection activities to evaluate road surface deteriorating performance and damage conditions. For instance, IRI is a field degradation performance measure often adopted and reported by transportation agencies to quantify the smoothness of roads. It is calculated based on the road's longitudinal profiles collected by a profiler attached to the inspecting vehicle. IRI is reported in units of inches per mile and has values ranging from 0 to ∞ [27]. The lower IRI value represents better road condition and vice versus. Due to the influence of various uncertain or unobserved factors, such as uncertain field environment and unobserved intrinsic material structure, the field degradation performance of a road evolves stochastically over time. To capture such degradation uncertainty, we consider the discrete-time Markov chains due to its practical convenience for maintenance decision making in discrete time points as well as its validity (i.e., Markov properties) justified in the existing field data analysis of road degradation data [28].

We begin with modeling the degradation performance of the road in the absence of maintenance activities. Denoting degradation state variable, s_t^{R}, $t = 1, \ldots, \mathrm{T}$, to represent the discretized states of the continuous service performance indicator (i.e., IRI) at time t, s_t^{R} can take different discrete values that reflect the condition of a road, i.e., $s_t^{\mathrm{R}} \in \mathbf{S}^{\mathrm{R}} = \{1,\ 2, \ldots, \mathrm{N}^{\mathrm{R}}\}$. "1" represents the perfect condition, and the larger value of s_t^{R} indicates a deteriorating road with poorer road condition, such as larger road roughness. "N^{R}" represents the

failure condition. We further denote the degradation transition matrix in the absence of maintenance activities as $\mathbf{P}_0^{\mathrm{R}} = \left[p_{0_{ij}}^{\mathrm{R}} \right]$, where its element on the i^{th} row and the j^{th} column can be written as $p_{0_{ij}}^{\mathrm{R}} = \Pr\left(s_{t+1}^{\mathrm{R}} = j \mid s_t^{\mathrm{R}} = i\right)$ and $p_{0_{ij}}^{\mathrm{R}} = 0$ when $i > j$. For non-zero elements in the transition matrix, they can be learned from the actual inspection data collected in the field. Specifically, for the road inspection and data collection purposes, the road network is divided into road sections where a road section is defined to be a road segment having uniform characteristics. Given the historical observed degradation data of the road network, we further denote n_{ij} as the number of road sections that move from state i to state j. Then the log-likelihood function $l\left(\boldsymbol{p}_0^{\mathrm{R}}\right)$ can be written as

$$l\left(\boldsymbol{p}_0^{\mathrm{R}}\right) = \log\Pr\left(s_1^{\mathrm{R}} = 1\right) + \sum_{i=1}^{\mathrm{N^R}} \sum_{j=1}^{\mathrm{N^R}} n_{ij} \log p_{0_{ij}}^{\mathrm{R}} \tag{1}$$

where $n_{ij} = \sum_{t=1}^{\mathrm{T}-1} \mathrm{I}(s_t^{\mathrm{R}} = i, s_{t+1}^{\mathrm{R}} = j)$, and $\mathrm{I}(\cdot)$ is the indicator function that has the value of 1 if $s_t^{\mathrm{R}} = i, s_{t+1}^{\mathrm{R}} = j$, and 0 otherwise. Based on the maximum likelihood estimation, the closed-form estimate for $p_{0_{ij}}^{\mathrm{R}}$, i.e., $\hat{p}_{0_{ij}}^{\mathrm{R}}$, can be described as

$$\hat{p}_{0_{ij}}^{\mathrm{R}} = \Pr\left(s_{t+1}^{\mathrm{R}} = j | s_t^{\mathrm{R}} = i\right) = \frac{n_{ij}}{n_i} \tag{2}$$

where $n_i = \sum_{j=1}^{\mathrm{N^R}} n_{ij}$ is the number of road sections in state $i, \forall i \in \mathbf{S}^{\mathrm{R}}$.

To further associate the performance degradation with different maintenance activities, we define road maintenance action at time t as $a_t^{\mathrm{R}} \in \mathbf{A}^{\mathrm{R}}$, where $\mathbf{A}^{\mathrm{R}}$ is a set of possible repair actions. In this paper, we consider the typical repair actions of "do nothing (DN)", "minor maintenance (MM)", and "perfect maintenance (PM)". For "MM", the road condition (i.e., state i) will be minimally restored to the previous degradation state (i.e., state $i-1$). For "PM", the road condition (i.e., state i) will be restored to the perfect condition, i.e., state "1". We further define a set of conditional probability matrix $\mathbf{P}^{\mathrm{R}}\left(a_t^{\mathrm{R}}\right) = \left[p_{ij}^{\mathrm{R}}\left(a_t^{\mathrm{R}}\right)\right], a_t^{\mathrm{R}} = \mathrm{DN}, \mathrm{MM}, \mathrm{PM}$, where $p_{ij}^{\mathrm{R}}\left(a_t^{\mathrm{R}}\right) = \Pr\left(s_{t+1}^{\mathrm{R}} = j | s_t^{\mathrm{R}} = i, a_t^{\mathrm{R}}\right)$. If the repair action is "DN"(i.e., $a_t^{\mathrm{R}} = \mathrm{DN}$), or the road is in perfect condition at time t ($s_t^{\mathrm{R}} = 1$), there is no maintenance needed, therefore, the transition probability $p_{ij}^{\mathrm{R}}\left(a_t^{\mathrm{R}}\right) = \Pr\left(s_{t+1}^{\mathrm{R}} = j | s_t^{\mathrm{R}} = i, a_t^{\mathrm{R}} = \mathrm{DN}\right) = p_{0_{ij}}^{\mathrm{R}}$. When repair action is "MM" or "PM", i.e., $a_t^{\mathrm{R}} = \mathrm{MM}$ or PM, $p_{ij}^{\mathrm{R}}\left(a_t^{\mathrm{R}}\right) = \Pr(s_{t+1}^{\mathrm{R}} = j | s_t^{\mathrm{R}} = i, a_t^{\mathrm{R}})$ can be explicitly written as

$$p_{ij}^{\mathrm{R}}\left(a_t^{\mathrm{R}}\right) = \sum_{\forall j' \in \mathbf{S}^{\mathrm{R}}} q_{ij'}\left(a_t^{\mathrm{R}}\right) \times p_{0_{j'j}}^{\mathrm{R}} \ , \tag{3}$$

and

$$q_{ij'}\left(a_t^{\mathrm{R}}\right) = \begin{cases} 1 \text{ if } a_t^{\mathrm{R}} = \mathrm{MM} \text{ and } j' = i-1 \\ 1 \text{ if } a_t^{\mathrm{R}} = \mathrm{PM} \text{ and } j' = 1 \\ 0 \text{ otherwise} \end{cases} . \tag{4}$$

2.1.2. Corrosion-induced pipe degradation performance modeling

Corrosion is one of the major failure causes for pipe breaks. Due to the influence of uncertain environmental conditions, such as soil salinity/pH/porosity, humidity, temperature, the corrosion process of the pipe is highly uncertain. To capture such corrosion-induced degradation uncertainty and characterize the evolution of corroded depth over time, we consider the Gamma process (GP), which is often applied in the existing literature as a good surrogate model to capture the stochastic corrosion process of in-service water pipes [29, 30]. It is noticed that, for illustration purposes, we use the widely accepted GP to capture corrosion-induced degradation of the pipe. For practical usage, if actual degradation data is available for the practitioners, different stochastic processes can be considered and the one with the best goodness-of-fit of actual data can be selected. Specifically, denoting $D(t)$ as the corrosion depth of the pipe at time $t \geq 0$, $D(t)$ can be characterized by a GP with the mean function of $\alpha(t)$ and scale parameter $\phi > 0$. $\alpha(t)$ describes the average evolution trend of the corrosion process. Meanwhile, ϕ controls the dispersion of the stochastic corrosion path around its mean function $\alpha(t)$. The expected corrosion depth of the pipe has been proven by many studies to follow the power law [31]. Therefore, the mean function $\alpha(t)$can be represented as $\alpha(t) = ct^v$, where $c > 0$ and $v > 0$ are constants. Based on the existing engineering knowledge, the power constant v is normally assumed to be known, while the constant c and scale parameter ϕ can be estimated using common statistical methods, such as maximum likelihood estimation [31]. The corrosion depth increment between time t and $t + \tau$, with its realization denoted as d, follows a Gamma distribution, i.e., $\Delta D(t) = D(t + \tau) - D(t) \sim \text{Ga}(\alpha(t + \tau) - \alpha(t), \phi)$ with the probability density function (PDF) given by,

$$f_{\Delta D(t)}(d; \alpha(t), \phi) = \frac{\phi^{\alpha(t+\tau)-\alpha(t)}}{\Gamma(\alpha(t + \tau) - \alpha(t))} d^{\alpha(t+\tau)-\alpha(t)-1} \exp(-\phi d) \tag{5}$$

Based on the corrosion process model characterized by the GP, to facilitate the maintenance-decision making, we further discretize the continuous state space of corrosion depth into several discrete states based on a series of cutting points, i.e., $0 \leq b_1 < b_2 < \cdots < b_{\text{N}^\text{P}}$. We further let $s_t^\text{P} \in \mathbf{S}^\text{P} = \{1, 2, \ldots, \text{N}^\text{P}\}$be the degradation state of pipe at time t with state "1" representing the perfect functioning state. The higher state value indicates a worsened degradation state. When the corroded depth exceeds pipe's wall thickness, the pipe break will occur and "N^P" is used to represent the failure state. Based on such discretization, denote the transition probability matrix as $\mathbf{P}_0^\text{P} = \left[p_{0_{ij}}^\text{P}\right]$, where its element $p_{0\,ij}^\text{P} = p_0^\text{P}\left(s_{t+1}^\text{P} = j | s_t^\text{P} = i\right); i, j \in \mathbf{S}^\text{P}$. $p_{0\,ij}^\text{P}$ represents the probability of pipe condition transferring from state i at the beginning of year t to state j at the beginning of year $t+1$. Due to the non-decreasing increment of corrosion depth in continuous scale (i.e., $j \geq i$ in the discrete case), $p_{0\,ij}^\text{P} = 0$ if $j < i$. To calculate such transition probability, we consider the Monte Carlo simulation to simulate a large number of realizations of the specified GP on the continuous

scale. Then the transition probability can be calculated from the simulated data by discretizing them into ranges representing different discrete states [32].

We further incorporate the maintenance actions into the corrosion-induced degradation probability. At each time point $t = 1, 2, \ldots, \mathrm{T}$, a variable $a_t^{\mathrm{P}} \in \mathbf{A}^{\mathrm{P}}$ represents the available maintenance action for the pipe in state s_t^{P}. Similar to Eqs. (3) and (4), three maintenance actions, namely, "DN", "MM", and "PM", are considered. "MM" will restore the corrosion-induced degradation state to its previous degradation state via repair actions, such as various corrosion control and protection activities (e.g., physical protection, cathodic protection) [33] to mitigate the corrosion damage, while "PM" will replace the pipe with a new pipe in the perfect condition. We further denote $\mathbf{P}^{\mathrm{P}}\left(a_t^{\mathrm{P}}\right) = \left[p_{ij}^{\mathrm{P}}\left(a_t^{\mathrm{P}}\right)\right]$, where $p_{ij}^{\mathrm{P}}\left(a_t^{\mathrm{P}}\right) = \Pr\left(s_{t+1}^{\mathrm{P}} = j | s_t^{\mathrm{P}} = i, a_t^{\mathrm{P}}\right)$ is a conditional probability quantity given different maintenance actions a_t^{P}, which can be explicitly written as

$$p_{ij}^{\mathrm{P}}\left(a_t^{\mathrm{P}}\right) = \begin{cases} p_{0_{ij}}^{\mathrm{P}} \text{ if } a_t^{\mathrm{P}} = \mathrm{DN} \text{ or } i = 1 \\ \sum_{\forall j' \in \mathbf{S}^{\mathrm{P}}} \; q_{ij'}\left(a_t^{\mathrm{P}}\right) \times p_{0_{j'j}}^{\mathrm{P}} \text{ if } a_t^{\mathrm{P}} \neq \mathrm{DN} \end{cases}, \tag{6}$$

and

$$q_{ij'}\left(a_t^{\mathrm{P}}\right) = \begin{cases} 1 \text{ if } a_t^{\mathrm{P}} = \mathrm{MM} \text{ and } j^{'} = i - 1 \\ 1 \text{ if } a_t^{\mathrm{P}} = \mathrm{PM} \text{ and } j^{'} = 1 \\ 0 \text{ otherwise} \end{cases}. \tag{7}$$

For illustration purposes without losing generality, three maintenance actions are considered in the above formulation. In practice, based on the actual need of local stakeholders, more detailed fidelity of maintenance actions can be considered by increasing the dimension of action space. For instance, for pipe repair, it is possible to consider both minor repair (e.g., pipe cleaning) and major repair (e.g., pipe lining) actions. Then the total number of actions for the pipe becomes 4, i.e., $\left|\mathbf{S}^{\mathrm{P}}\right| = 4$. $q_{ij'}\left(a_t^{\mathrm{P}}\right)$ in Eq. (7) can be updated by modeling the effects of minor and major pipe repairs. Eq. (6) is generic and will remain the same by using the updated $q_{ij'}\left(a_t^{\mathrm{P}}\right)$.

2.1.3. Adjusted pipe failure probability modeling under the traffic-load effect

In addition to the corrosion-induced gradual failure mode described in Section 2.1.2, another important failure mode for pipe break is the sudden failure resulting from the traffic loading exerted from the co-located road. When the applied stress (resulting from the traffic load of the road) on the underneath pipe exceeds the pipe tensile strength, sudden failure of pipe break will occur. Thus, the overall failure probability of the pipe needs to take into account the above two competing failure models. Denoting $x_t^{\mathrm{f}} \in \{0, 1\}$ as a binary variable to represent the sudden failure state of a pipe resulting from traffic-load effect at time t, state "1" represents "failure" and state "0" represents "no failure". Letting $p_{\mathrm{d}_i} = \Pr\left(x_{t+1}^{\mathrm{f}} = 1 | s_t^{\mathrm{P}} = i, x_t^{\mathrm{f}}, \boldsymbol{\theta}^{\mathrm{R}}\right), i \in \mathbf{S}^{\mathrm{P}}$ represent the traffic-load-induced (TLI) sudden failure probability, it captures the physical dependence existing between the co-located road and pipe. Several factors may potentially influence

p_{d_i}. First, the current degradation states of pipe will affect p_{d_i}. The pipe at a worsened corrosion-induced degradation state has a significantly thinner wall thickness. Since drinking water pipe is considered in this study, the thinner wall thickness will not affect the flow capacity of the pipe, however, it will lower the sustained capacity of pipe from stress. Second, there are also other TLI influencing factors (represented by $\boldsymbol{\theta}^{\mathrm{R}}$), such as traffic load and the design parameter between road and pipe. Traffic load may vary considerably due to the influence of different types of vehicles (ranging from passenger cars to heavy trucks), and thus may affect p_{d_i} differently. The design of pipe installation can also affect p_{d_i}. Particularly, the installation process will affect the depth of cover defined as the distance from the top of the pipe to the road surface. The closer the pipe is installed to the road surface (i.e., less depth of cover), the higher risk of pipe break may exist due to the heavy traffic above. Beside the installation process, the road degradation condition may also affect the depth of cover from the pipe to the surface of the road. However, the road has different layers, and the top layer which reflects the condition of the road is much thinner than others. Therefore, the effect from the installation process on the pipe depth of cover can be much more significant than that from the condition state of the road. For this reason, the effect of road condition state on p_{d_i} can be neglected.

To quantify p_{d_i} by taking into account the impact of these aforementioned factors, there are several challenges. First, buried water pipe generally traverses through different types of soil conditions, and geological conditions. Second, water pipes are made with a variety of different materials, which have different response behavior under stress. Lastly, when the pipe is subjected to compression due to outside load, fault motion and material deformation can happen within the pipe itself. Hence, using an analytical modeling approach for evaluating the effect of traffic load on pipe can be very challenging, and make the model too complex for practical applications. Besides, because of too many inputs (i.e., soil conditions, pipe materials), the approach using empirical experiments can be expensive to test the effect of traffic load on pipe under different scenarios. Thus, by utilizing the computational advancement in numerical modeling, FEA is considered in this paper to evaluate the maximum stress on the pipe under the load of different types of vehicles. A pipe is considered to be broken if its stress state exceeds the strength value of the material used to make the pipe. The details of modeling parameters (e.g., soil layers, material) can be found in the recently developed FEA model using ANSYS software [34]. We utilize this model to evaluate the influence of traffic load on pipe failure under different loading scenarios (see Table 4 for details of loading scenarios).

After evaluating p_{d_i} based on FEA, we will model the adjusted pipe failure probability under the traffic-load effect by taking into account the two competing failure modes, namely the corrosion-induced gradual failure mode and TLI sudden failure mode. Fig. 2 describes the relationship between the overall failure probability of pipe with these two competing failure modes. Assuming the two competing failure modes are independent, the adjusted failure probability can be generically expressed as

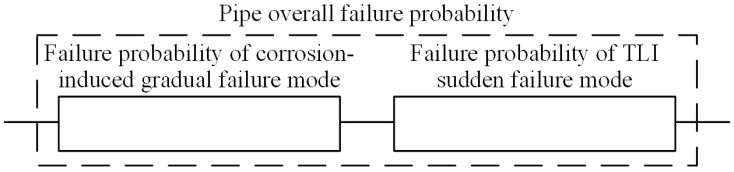

Figure 2: Illustrative diagram of pipe failure probability with multiple competing failure causes.

$$
\begin{aligned}
&\Pr\Big(s_{t+1}^{\mathrm{P}} = \mathrm{N}^{\mathrm{P}} \text{ or } x_{t+1}^{\mathrm{f}} = 1 | s_t^{\mathrm{P}} = i, x_t^{\mathrm{f}}, \boldsymbol{\theta}^{\mathrm{R}}\Big) \\
&= 1 - \Pr(\text{No corrosion failure and no sudden failure between } t \text{ and } t+1) \\
&= 1 - \Pr(\text{No corrosion failure from } t \text{ to } t+1) \\
&\qquad \times \Pr(\text{No sudden failure from } t \text{ to } t+1) \\
&= 1 - \big[1 - \Pr\big(s_{t+1}^{\mathrm{P}} = \mathrm{N}^{\mathrm{P}} | s_t^{\mathrm{P}} = i\big)\big] \times \Big[1 - \Pr\Big(x_{t+1}^{\mathrm{f}} = 1 | x_t^{\mathrm{f}}, s_t^{\mathrm{P}} = i, \boldsymbol{\theta}^{\mathrm{R}}\Big)\Big]
\end{aligned} \tag{8}
$$

Based on Eq. (8), the adjusted pipe failure probability can be more explicitly evaluated under different scenarios of sudden failure states. When $x_t^{\mathrm{f}} = 0$ and $x_{t+1}^{\mathrm{f}} = 1$, there is $\Pr\Big(x_{t+1}^{\mathrm{f}} = 1 | s_t^{\mathrm{P}} = i, x_t^{\mathrm{f}} = 0, \boldsymbol{\theta}^{\mathrm{R}}\Big) = p_{\mathrm{d}_i}, i \in \mathbf{S}^{\mathrm{P}}$ and we will have $\Pr\Big(s_{t+1}^{\mathrm{P}} = \mathrm{N}^{\mathrm{P}} \text{ or } x_{t+1}^{\mathrm{f}} = 1 | s_t^{\mathrm{P}} = i, x_t^{\mathrm{f}} = 0, \boldsymbol{\theta}^{\mathrm{R}}\Big) = 1 - \Big(1 - p_{0_{i\mathrm{N}^{\mathrm{P}}}}^{\mathrm{P}}\Big)(1 - p_{\mathrm{d}_i})$. When $x_t^{\mathrm{f}} = 1$ and $x_{t+1}^{\mathrm{f}} = 0$, there are $\Pr\Big(x_{t+1}^{\mathrm{f}} = 0 | s_t^{\mathrm{P}} = i, x_t^{\mathrm{f}} = 1, \boldsymbol{\theta}^{\mathrm{R}}\Big) = 0$, and $\Pr\Big(s_{t+1}^{\mathrm{P}} = \mathrm{N}^{\mathrm{P}} \text{ or } x_{t+1}^{\mathrm{f}} = 0 | s_t^{\mathrm{P}} = i, x_t^{\mathrm{f}} = 1, \boldsymbol{\theta}^{\mathrm{R}}\Big) = p_{0_{i\mathrm{N}^{\mathrm{P}}}}^{\mathrm{P}}$. When $x_t^{\mathrm{f}} = 1$ and $x_{t+1}^{\mathrm{f}} = 1$, which indicates the sudden failure occurs at time t and the pipe remains broken till time $t+1$, there is $\Pr\Big(x_{t+1}^{\mathrm{f}} = 1 | s_t^{\mathrm{P}} = i, x_t^{\mathrm{f}} = 1, \boldsymbol{\theta}^{\mathrm{R}}\Big) = 1$ and we will have $\Pr\Big(s_{t+1}^{\mathrm{P}} = \mathrm{N}^{\mathrm{P}} \text{ or } x_{t+1}^{\mathrm{f}} = 1 | s_t^{\mathrm{P}} = i, x_t^{\mathrm{f}} = 1, \boldsymbol{\theta}^{\mathrm{R}}\Big) = 1$.When $x_t^{\mathrm{f}} = x_{t+1}^{\mathrm{f}} = 0$, the pipe degradation process is only affected by the corrosion. The pipe state transition probability $\Pr\Big(s_{t+1}^{\mathrm{P}} = j \neq \mathrm{N}^{\mathrm{P}}, x_{t+1}^{\mathrm{f}} = 0 | s_t^{\mathrm{P}} = i, x_t^{\mathrm{f}} = 0, \boldsymbol{\theta}^{\mathrm{R}}\Big)$ is $p_{0_{ij}}^{\mathrm{P}}$ and the adjusted failure probability can be directly obtained from state transition probability matrix $\mathbf{P}_0^{\mathrm{P}}$. For all the scenarios, we can observe that $\Pr\Big(s_{t+1}^{\mathrm{P}} = \mathrm{N}^{\mathrm{P}} \text{ or } x_{t+1}^{\mathrm{f}} = 1 | s_t^{\mathrm{P}} = i, x_t^{\mathrm{f}}, \boldsymbol{\theta}^{\mathrm{R}}\Big) \geq p_{0_{i\mathrm{N}^{\mathrm{P}}}}^{\mathrm{P}}$. Therefore, without considering the physical dependence from road to pipe, the overall pipe failure probability will be underestimated.

Given the results from Eq. (8), we further explore the state transition probability of pipe under traffic-load effect and the effect of maintenance actions a_t^{P}, denoted as $p_{ij}^{\mathrm{f}}\big(a_t^{\mathrm{P}}\big) = \Pr\Big(s_{t+1}^{\mathrm{P}} = j, x_{t+1}^{\mathrm{f}} | s_t^{\mathrm{P}} = i, x_t^{\mathrm{f}}, a_t^{\mathrm{P}}, \boldsymbol{\theta}^{\mathrm{R}}\Big)$. When no failure occurs, i.e., $s_{t+1}^{\mathrm{P}} \in \mathbf{S}^{\mathrm{P}} \backslash \big\{\mathrm{N}^{\mathrm{P}}\big\}$ and $x_t^{\mathrm{f}} = x_{t+1}^{\mathrm{f}} = 0$, there is $p_{ij}^{\mathrm{f}}\big(a_t^{\mathrm{P}}\big) = p_{ij}^{\mathrm{P}}\big(a_t^{\mathrm{P}}\big)$, where

$p_{ij}^{\mathrm{P}}\left(a_t^{\mathrm{P}}\right)$ can be calculated from Eq. (6). When failure occurs, $p_{i\mathrm{N^P}}^{\mathrm{f}}\left(a_t^{\mathrm{P}}\right)$can be expressed as

$$\begin{aligned} & p_{i\mathrm{N^P}}^{\mathrm{f}}\left(a_t^{\mathrm{P}}\right)=\Pr\left(s_{t+1}^{\mathrm{P}}=\mathrm{N^P} \text{ or } x_{t+1}^{\mathrm{f}}=1 | s_t^{\mathrm{P}}=i, x_t^{\mathrm{f}}, \boldsymbol{\theta}^{\mathrm{R}}\right) \\ & =\left\{\begin{array}{l} 1-\left(1-p_{0_{i\mathrm{N^P}}}^{\mathrm{P}}\right)\left(1-p_{\mathrm{d}_i}\right) \text{ if } a_t^{\mathrm{P}}=\mathrm{DN} \\ \sum_{\forall j' \in \mathbf{S}^{\mathrm{R}}} q_{ij'}\left(a_t^{\mathrm{P}}\right) \times\left\{1-\left(1-p_{0_{j'\mathrm{N^P}}}^{\mathrm{P}}\right)\left(1-p_{\mathrm{d}_{j'}}\right)\right\} \text{ if } a_t^{\mathrm{P}} \neq \mathrm{DN} \end{array}, i \in \mathbf{S}^{\mathrm{P}}\right. \end{aligned} \tag{9}$$

where $q_{ij'}\left(a_t^{\mathrm{P}}\right)$ has been defined in Eq. (7).

2.2. Maintenance optimization modeling for co-located road and pipe with operational dependency

In this section, we will formulate the joint proactive maintenance planning model for the co-located road and pipe by taking into account the operational dependency. Such dependency can be reflected in two aspects, (1) repaving and its influence on operational costs of maintenance; (2) disruption of pipe maintenance and its influence on road user costs. Let $\boldsymbol{s}_t$ and $\boldsymbol{a}_t$ be the joint condition states and the associated maintenance actions at time t of the co-located road and pipe, respectively. $\boldsymbol{s}_t$ and $\boldsymbol{a}_t$ can be specifically defined as

$$\begin{aligned} & \boldsymbol{s}_t \in \mathbf{S}=\mathbf{S}^{\mathrm{R}} \times \mathbf{S}^{\mathrm{P}}=\left\{\left(s_t^{\mathrm{R}}, s_t^{\mathrm{P}}\right): s_t^{\mathrm{R}} \in \mathbf{S}^{\mathrm{R}}, s_t^{\mathrm{P}} \in \mathbf{S}^{\mathrm{P}}\right\}, t=1, \ldots, \mathrm{T} \\ & \boldsymbol{a}_t \in \mathbf{A}=\mathbf{A}^{\mathrm{R}} \times \mathbf{A}^{\mathrm{P}}=\left\{\left(a_t^{\mathrm{R}}, a_t^{\mathrm{P}}\right): a_t^{\mathrm{R}} \in \mathbf{A}^{\mathrm{R}}, a_t^{\mathrm{P}} \in \mathbf{A}^{\mathrm{P}}\right\}, t=1, \ldots, \mathrm{T} \end{aligned} \tag{10}$$

where, $|\bullet|$ represents the cardinality of a set. The state space $\mathbf{S}$ contains $\left|\mathbf{S}^{\mathrm{R}}\right| \times\left|\mathbf{S}^{\mathrm{P}}\right|$ joint condition states and the action space $\mathbf{A}$ has $\left|\mathbf{A}^{\mathrm{R}}\right| \times\left|\mathbf{A}^{\mathrm{P}}\right|$ joint maintenance actions. We will discuss the cost components of maintenance costs and traffic control costs in Section 2.2.1, and user costs in Section 2.2.2 for the joint states due to the operational dependency between road and pipe.

2.2.1. Maintenance costs and traffic control costs modeling

Denoting C_{m} as the total maintenance costs for the co-located road and pipe section, it includes cost components, such as labor, tools, and materials costs for repairing road and pipe. Due to the co-location, there are opportunities for cost saving if the road and pipe can be jointly maintained during the same time period. Particularly, repaving costs can be avoided if road and pipe maintenance actions are jointly determined. Repaving costs refers to the amount of surface material, machine, and labor used to return the surface to its original condition when the activities on the pipe are done. Besides, the pavement covering the pipe is normally a smaller area inside the main road. Therefore, in the conventional road and pipe repairs scheduled at two different non-overlapping time periods separately, additional machine and labor costs need to be spent

for road repaving. When jointly repairing road and pipe during the same time period, the repaving can be taken care of by road maintenance crew as part of road maintenance activity. For this reason, the total maintenance costs can be written as

$$C_{\mathrm{m}}(\boldsymbol{s}_t, \boldsymbol{a}_t) = C_{\mathrm{m}}\big(s_t^{\mathrm{R}}, a_t^{\mathrm{R}}\big) + C_{\mathrm{m}}\big(s_t^{\mathrm{P}}, a_t^{\mathrm{P}}\big) - \mathrm{I}_{\left\{a_t^{\mathrm{R}} \neq \mathrm{DN} \ \&\ a_t^{\mathrm{P}} \neq \mathrm{DN}\right\}} \times C\mathrm{r} \tag{11}$$

where, $C_{\mathrm{m}}\big(s_t^{\mathrm{R}}, a_t^{\mathrm{R}}\big)$ and $C_{\mathrm{m}}\big(s_t^{\mathrm{P}}, a_t^{\mathrm{P}}\big)$ are maintenance costs for the road and pipe, respectively. $C\mathrm{r}$ is the repaving costs. $\mathrm{I}_{\left\{a_t^{\mathrm{R}} \neq \mathrm{DN}\ \& a_t^{\mathrm{P}} \neq \mathrm{DN}\right\}}$ is an indicator function, which implies that when both road and pipe have higher maintenance activities than "DN", they can be arranged in the same time period and the extra repaving costs can be avoided.

The second cost saving opportunity for jointly maintaining co-located road and pipe is the total traffic control costs. Denoting $C_{\mathrm{tc}}\big(a_t^{\mathrm{R}}\big)$ and $C_{\mathrm{tc}}\big(a_t^{\mathrm{P}}\big)$ as the traffic control costs for road and pipe, respectively, they include all costs related to the signs, tools, vehicles, and people to control the traffic passing by the maintenance area. It is observed that the traffic control task only depends on the maintenance level and thus is action dependent. Further denoting T^{R} and T^{P} as the amount of time needed for maintaining road and pipe, respectively, in the traditional maintenance planning when both road and pipe are repaired in two different time periods separately, the total traffic control costs $C_{\mathrm{tc}}(\boldsymbol{a}_t)$will cover the whole length of two maintenance time periods, i.e., $T^{\mathrm{R}} + T^{\mathrm{P}}$, and become $C_{\mathrm{tc}}(\boldsymbol{a}_t) = C_{\mathrm{tc}}\big(a_t^{\mathrm{R}}\big) + C_{\mathrm{tc}}\big(a_t^{\mathrm{P}}\big)$. However, since road and pipe are co-located, they share the same traffic area. If repairing them in the same time period, the one (e.g., pipe) that has shorter maintenance time can use the same traffic control as the other one (e.g., road) that has a longer maintenance time. Then the total traffic control costs can be reduced as

$$C_{\mathrm{tc}}(\boldsymbol{a}_t) = \max\big(C_{\mathrm{tc}}\big(a_t^{\mathrm{R}}\big),\ C_{\mathrm{tc}}\big(a_t^{\mathrm{P}}\big)\big). \tag{12}$$

2.2.2. User costs modeling

Another cost saving opportunity due to the operational dependency between road and pipe is related to the user costs, denoted as $C_{\mathrm{u}}(\boldsymbol{s}_t, \boldsymbol{a}_t)$. $C_{\mathrm{u}}(\boldsymbol{s}_t, \boldsymbol{a}_t)$ can be further decomposed into two cost components, namely the short-term user costs $C_{\mathrm{ust}}(\boldsymbol{s}_t, \boldsymbol{a}_t)$, and the long-term user costs $C_{\mathrm{ult}}(\boldsymbol{s}_t, \boldsymbol{a}_t)$. $C_{\mathrm{ust}}(\boldsymbol{s}_t, \boldsymbol{a}_t)$ involves the traffic delay costs caused by traffic blockage due to the maintenance activities (e.g., road and pipe maintenance). $C_{\mathrm{ult}}(\boldsymbol{s}_t, \boldsymbol{a}_t)$ represents the cumulative user costs caused by the condition of the road and pipe from the last maintenance to the next one, including both the road and water users' costs due to various negative consequences (e.g., traffic delay, water unmet demand) of the deteriorating road and pipe. They will be modeled explicitly later in this subsection.

Considering the traditional maintenance approach when road and pipe are maintained separately during different times, there will be a total of $T^{\mathrm{R}} + T^{\mathrm{P}}$

traffic blockage time on the co-located road and pipe section. By jointly repairing co-located road and pipe during the same time period, the traffic blockage time will be reduced and equal to the time of the longer maintenance activity (i.e., $\max(T^{\mathrm{R}}, T^{\mathrm{P}})$), and therefore reduce the overall short-term user costs. However, when maintained jointly, the maintenance of the pipe will potentially affect the users of surrounding road sections depending on the actual placement position of the pipe. Fig. 3 gives several examples of typical intersections. In addition to the selected road under repair (marked in gray areas), there may exist neighboring road sections (marked in white areas). We let β represent the total number of road sections, including both the road under repair as well as its neighboring road sections connected through the intersections. Although the road maintenance (in gray area) will not affect these neighboring road sections, depending on the position where the pipe is buried, the maintenance activity of pipe will affect these neighboring road sections. β can be also viewed as the propagated effect, which quantifies the influence of pipe maintenance activities on the total number of road sections (i.e., $\beta \geq 1$) in the co-located neighboring area. To clearly explain the impact of propagated effect β on $C_{\mathrm{ust}}(\boldsymbol{s}_t, \boldsymbol{a}_t)$, different scenarios, i.e., $T^{\mathrm{R}} \geq T^{\mathrm{P}}$ and $T^{\mathrm{R}} < T^{\mathrm{P}}$, will be considered.

When $T^{\mathrm{R}} \geq T^{\mathrm{P}}$, the total traffic blockage time period can be divided into two parts, namely the T^{P} and $T^{\mathrm{R}} - T^{\mathrm{P}}$. The short-term user costs can be explicitly written as

$$\begin{aligned} C_{\mathrm{ust}}(\boldsymbol{s}_t, \boldsymbol{a}_t) = C^{\mathrm{R}}_{\mathrm{u_{maint}}}\left(s_t^{\mathrm{R}}, a_t^{\mathrm{R}}\right) \times T^{\mathrm{P}} + (\beta - 1) \times C^{\mathrm{P}}_{\mathrm{u_{prop}}}\left(s_t^{\mathrm{P}}, a_t^{\mathrm{P}}\right) \times T^{\mathrm{P}} \\ + C^{\mathrm{R}}_{\mathrm{u_{maint}}}\left(s_t^{\mathrm{R}}, a_t^{\mathrm{R}}\right) \times \left(T^{\mathrm{R}} - T^{\mathrm{P}}\right) \end{aligned} \tag{13}$$

where $C^{\mathrm{R}}_{\mathrm{u_{maint}}}\left(s_t^{\mathrm{R}}, a_t^{\mathrm{R}}\right)$ and $C^{\mathrm{P}}_{\mathrm{u_{prop}}}\left(s_t^{\mathrm{P}}, a_t^{\mathrm{P}}\right)$ are the road user costs per day caused by road maintenance and pipe maintenance activities, respectively. They can be calculated as

$$C^{\mathrm{R}}_{\mathrm{u_{maint}}}\left(s_t^{\mathrm{R}}, a_t^{\mathrm{R}}\right) = D^{\mathrm{R}}_{\mathrm{maint}}\left(s_t^{\mathrm{R}}, a_t^{\mathrm{R}}\right) \times TF \times c_1 \tag{14}$$

$$C^{\mathrm{P}}_{\mathrm{u_{prop}}}\left(s_t^{\mathrm{P}}, a_t^{\mathrm{P}}\right) = D^{\mathrm{P}}_{\mathrm{maint}}\left(s_t^{\mathrm{P}}, a_t^{\mathrm{P}}\right) \times TF \times c_1 \tag{15}$$

where $D^{\mathrm{R}}_{\mathrm{maint}}\left(s_t^{\mathrm{R}}, a_t^{\mathrm{R}}\right)$ and $D^{\mathrm{P}}_{\mathrm{maint}}\left(s_t^{\mathrm{P}}, a_t^{\mathrm{P}}\right)$ (in hours/vehicle/day) are the total delay time of a vehicle caused by one day of maintenance activity on road and pipe, respectively. TF (in vehicles/day) is the average total traffic flow operating through the co-located road and pipe section per day. c_1 (in dollars/hour) is the monetary amount equivalent to the cost per hour for the delay of vehicles passing through the section under maintenance [35]. As shown in Eq. (13), the first and second terms represent the short-term user costs for the first time period with a duration T^{P}. During this time period, both the co-located pipe and road are repaired. Since the area of the pipe is significantly smaller than the road, the impact of the pipe maintenance to road users of the co-located road section will be neglected during the road maintenance time. Thus, $C^{\mathrm{R}}_{\mathrm{u_{maint}}}\left(s_t^{\mathrm{R}}, a_t^{\mathrm{R}}\right) \times$

T^{P} represents the short-term user costs of the co-located road under repair. Meanwhile, $(\beta-1)\times C^{\mathrm{P}}_{\mathrm{u_{prop}}}\left(s^{\mathrm{P}}_t, a^{\mathrm{P}}_t\right)\times T^{\mathrm{P}}$ represents the total short-term user costs in the neighboring road sections due to pipe maintenance. After pipe repair is completed, the third term $C^{\mathrm{R}}_{\mathrm{u_{maint}}}\left(s^{\mathrm{R}}_t, a^{\mathrm{R}}_t\right)\times\left(T^{\mathrm{R}}-T^{\mathrm{P}}\right)$ represent the short-term user costs in the remaining time period with a duration $T^{\mathrm{R}}-T^{\mathrm{P}}$ due to road maintenance.

Similarly, when the road maintenance is shorter than the pipe maintenance, i.e., $T^{\mathrm{R}}<T^{\mathrm{P}}$, the corresponding short-term user costs can be explicitly written as

$$\begin{aligned}C_{\mathrm{ust}}(\boldsymbol{s}_t,\boldsymbol{a}_t)=C^{\mathrm{R}}_{\mathrm{u_{maint}}}\left(s^{\mathrm{R}}_t,a^{\mathrm{R}}_t\right)\times T^{\mathrm{R}}+(\beta-1)\times C^{\mathrm{P}}_{\mathrm{u_{prop}}}\left(s^{\mathrm{P}}_t,a^{\mathrm{P}}_t\right)\times T^{\mathrm{R}}\\+\beta\times C^{\mathrm{P}}_{\mathrm{u_{prop}}}\left(s^{\mathrm{P}}_t,a^{\mathrm{P}}_t\right)\times\left(T^{\mathrm{P}}-T^{\mathrm{R}}\right).\end{aligned}\tag{16}$$

As shown in Eq. (16), one of the key differences from Eq. (13) is that after the road maintenance is completed, the remaining pipe maintenance will cause traffic blockage for both co-located and surrounding road sections, which is represented by $\beta\times C^{\mathrm{P}}_{\mathrm{u_{prop}}}\left(s^{\mathrm{P}}_t,a^{\mathrm{P}}_t\right)\times\left(T^{\mathrm{P}}-T^{\mathrm{R}}\right)$.

After road and pipe maintenance is completed at the beginning of this year, both road and pipe will continue to degrade and cause additional long-term user costs before the maintenance actions are performed in the next year. As defined earlier in this section, $C_{\mathrm{ult}}(\boldsymbol{s}_t,\boldsymbol{a}_t)$ represents the expected annual long-term users costs, which can be explicitly calculated as

$$\begin{aligned}&C_{\mathrm{ult}}\left(\boldsymbol{s}_t,x^{\mathrm{f}}_t,\boldsymbol{a}_t\right)\\&=\sum_{\boldsymbol{s}_{t+1}\in\mathbf{S},x^{\mathrm{f}}_{t+1}\in\{0,1\}}\Pr\left(\boldsymbol{s}_{t+1},x^{\mathrm{f}}_{t+1}|\boldsymbol{s}_t,x^{\mathrm{f}}_t,\boldsymbol{a}_t,\boldsymbol{\theta}^{\mathrm{R}}\right)\left(C^{\mathrm{R}}_{\mathrm{u}}\left(s^{\mathrm{R}}_{t+1}\right)+C^{\mathrm{P}}_{\mathrm{u}}\left(s^{\mathrm{P}}_{t+1}\right)\right)\end{aligned}\tag{17}$$

where $\Pr\left(\boldsymbol{s}_{t+1},x^{\mathrm{f}}_{t+1}|\boldsymbol{s}_t,x^{\mathrm{f}}_t,\boldsymbol{a}_t,\boldsymbol{\theta}^{\mathrm{R}}\right)$ is the joint transition probability which characterizes the performance degradation of the co-located road and pipe (and will be calculated in the next section, e.g., Eq. (20)). $C^{\mathrm{R}}_{\mathrm{u}}(s^{\mathrm{R}}_t)$ represents the annual cost that vehicle owners/drivers must pay when operating on the road with condition s^{R}_t. This user cost includes the cost due to the delay time of the road user when driving through the road section and the depreciation cost that the drivers must pay for their vehicle due to the road condition such as maintaining/repairing and fuel costs. $C^{\mathrm{R}}_{u}(s^{\mathrm{R}}_t)$ can be explicitly written as

$$C^{\mathrm{R}}_{\mathrm{u}}\left(s^{\mathrm{R}}_t\right)=D_{\mathrm{opt}}(\boldsymbol{s}_t)\times TF\times T_{\mathrm{e}}\times c_2+D_{\mathrm{opt}}(\boldsymbol{s}_t)\times TF\times T_{\mathrm{e}}\times c_3\tag{18}$$

where $D_{\mathrm{opt}}(\boldsymbol{s}_t)$ (in hours/vehicle/day) the total delayed time per day of a vehicle when operating through the road section and T_{e} (in days) is the length of a decision epoch (e.g., $T_{\mathrm{e}}=365$). c_2 (dollars/hour) is the monetary amount equivalent to the cost per hour for the delay of vehicles [35]. c_3 (dollars/hour) is

the cost that vehicle users must pay for fuel/maintaining/repairing the vehicles to run on the road section. For calculation purposes, this cost has been estimated to the monetary amount of the cost per hour for the delay of vehicles [35].

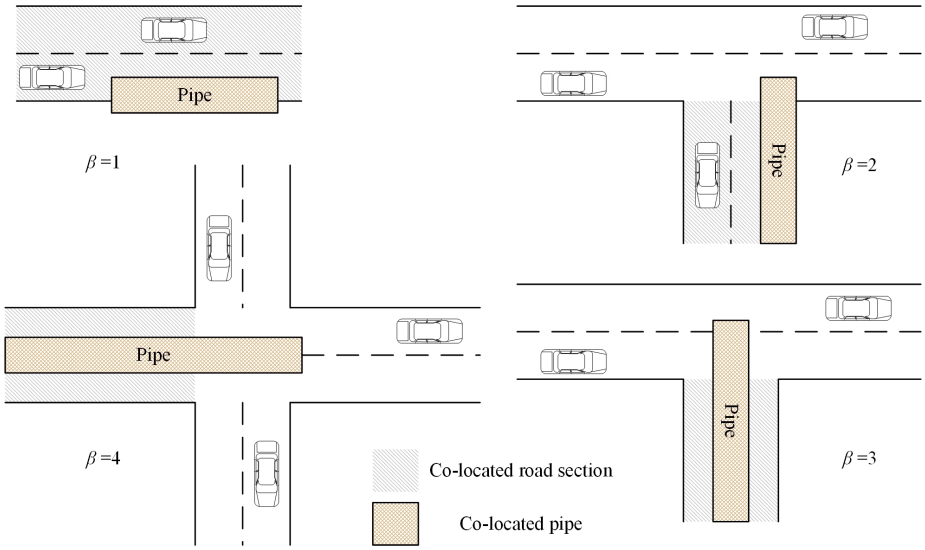

Figure 3: Different scenarios of propagated effect.

$C_{\mathrm{u}}^{\mathrm{P}}(s_t^{\mathrm{R}})$ represents the long-term water user costs, such as inconvenience caused by water unmet demand, water loss due to pipe condition, and possible water contamination during pipe break. To convert them into the equivalent monetary quantities, we consider the empirical formula proposed by Walski and Pelliccia [36], where the user costs can be equivalently written as a weight coefficient ρ multiplying the pipe maintenance cost $C_{\mathrm{m}}\left(s_t^{\mathrm{P}}\right)$. The higher the value of ρ, the more significant the water user costs will be. For instance, if the pipe is new and has minimal impact to water users, then ρ can be as low as 0. Meanwhile, the annual user costs for a pipe in a worsened condition can be more than 50% of its maintenance cost (i.e., $\rho \geq 0.5$).

2.2.3. Joint maintenance optimization

After modeling the specific cost components by taking into account the operational dependency from pipe to road, the overall joint maintenance planning model can be specifically formulated using Markov decision process (MDP) as follows. Considering a T-year planning horizon, the stakeholders will periodically evaluate the degradation performance of the co-located road and pipe at discrete times $t_0+(t-1)\times\Delta t, t=1,\ldots,\mathrm{T}$ (e.g., beginning of year t) and determine the maintenance decision for year t, where t_0 is the beginning of the entire planning horizon and Δt is a fixed time duration (e.g., year). Both the state vector $\boldsymbol{s}_t$ and action vector $\boldsymbol{a}_t$ are defined in Eq. (10). The joint maintenance planning model can be formulated to minimize the total expected long-run cost

as

$$V_{\pi}^{*}\left(\boldsymbol{s}_t, x_t^{\mathrm{f}}\right) = \min_{\boldsymbol{a}_t \in \mathbf{A}} \{C_{\mathrm{insp}} + C_{\mathrm{m}}(\boldsymbol{s}_t, \boldsymbol{a}_t) + C_{\mathrm{tc}}(\boldsymbol{a}_t) + C_{\mathrm{u}}(\boldsymbol{s}_t, \boldsymbol{a}_t) + \sum_{\boldsymbol{s}_{t+1} \in \mathbf{S}, x_{t+1}^{\mathrm{f}} \in \{0,1\}} \Pr(\boldsymbol{s}_{t+1} = j, x_{t+1}^{\mathrm{f}} | \boldsymbol{s}_t = i, x_t^{\mathrm{f}}, \boldsymbol{a}_t, \boldsymbol{\theta}^{\mathrm{R}}) \gamma V_{\pi}^{*}\left(\boldsymbol{s}_{t+1}, x_{t+1}^{\mathrm{f}}\right)\}, \quad (19)$$
$$t = 1, \ldots, \mathrm{T}-1$$

where $V_{\pi}^{*}\left(\boldsymbol{s}_t, x_t^{\mathrm{f}}\right)$ is the minimum total expected long-run costs given states $\boldsymbol{s}_t, x_t^{\mathrm{f}}$ and the maintenance policy π from year t to the end of the planning horizon. It consists of five additive terms in Eq. (19). The first term C_{insp} is the inspection costs of road and pipe of each decision epoch. It is noted that the costs for inspecting road and pipe condition (i.e., $C_{\mathrm{insp}}^{\mathrm{R}}$ and $C_{\mathrm{insp}}^{\mathrm{P}}$ respectively) are assumed to be fixed quantities regardless of the road and pipe condition. The second and third terms, i.e., $C_{\mathrm{m}}(\boldsymbol{s}_t, \boldsymbol{a}_t)$ and $C_{\mathrm{tc}}(\boldsymbol{a}_t)$, can be explicitly calculated based on Eqs. (11) and (12), respectively. The calculation of the fourth term $C_{\mathrm{u}}(\boldsymbol{s}_t, \boldsymbol{a}_t)$ can be found in Section 2.2.2. The fifth summation term quantifies the minimum expected long-run cost from year $t+1$ to the end of the planning horizon given all possible state scenarios at year $t+1$, where γ is the discount factor $(0 \leq \gamma \leq 1)$, and $V_{\pi}^{*}\left(\boldsymbol{s}_{t+1}, x_{t+1}^{\mathrm{f}}\right)$ quantifies the expected long-run cost from year $t+1$ to the end given states $\boldsymbol{s}_{t+1}$, and x_{t+1}^{f}. $\Pr\left(\boldsymbol{s}_{t+1} = j, x_{t+1}^{\mathrm{f}} | \boldsymbol{s}_t = i, x_t^{\mathrm{f}}, \boldsymbol{a}_t, \boldsymbol{\theta}^{\mathrm{R}}\right)$ is the joint state transition probability characterizing the performance degradation of the co-located road and pipe by incorporating the impact of the traffic load effect to the pipe's deterioration, which can be written as

$$\Pr\left(\boldsymbol{s}_{t+1} = j, x_{t+1}^{\mathrm{f}} \;\middle|\; \boldsymbol{s}_t = i, x_t^{\mathrm{f}}, \boldsymbol{a}_t, \boldsymbol{\theta}^{\mathrm{R}}\right) = p_{i^{\mathrm{R}} j^{\mathrm{R}}}^{\mathrm{R}}\left(a_t^{\mathrm{R}}\right) \times p_{i^{\mathrm{P}} j^{\mathrm{P}}}^{\mathrm{f}}\left(a_t^{\mathrm{P}}\right)$$
$$\forall \boldsymbol{s}_t \in \mathbf{S}; \boldsymbol{a}_t \in \mathbf{A}; x_t^{\mathrm{f}} \in \{0,1\}; i^{\mathrm{R}}, j^{\mathrm{R}} \in \mathbf{S}^{\mathrm{R}}; i^{\mathrm{P}}, j^{\mathrm{P}} \in \mathbf{S}^{\mathrm{P}}; a_t^{\mathrm{R}} \in \mathbf{A}^{\mathrm{R}}; a_t^{\mathrm{P}} \in \mathbf{A}^{\mathrm{P}}; \quad (20)$$
$$t = 1, \ldots, \mathrm{T}-1.$$

where $p_{i^{\mathrm{R}} j^{\mathrm{R}}}^{\mathrm{R}}\left(a_t^{\mathrm{R}}\right)$ and $p_{i^{\mathrm{P}} j^{\mathrm{P}}}^{\mathrm{f}}\left(a_t^{\mathrm{P}}\right)$ can be calculated from Eqs. (3) and (9), respectively. To solve the proposed optimization model of finite-horizon MDP, we consider the popular method of backward induction algorithm.

3. Real case study

3.1. Problem setup

3.1.1. Models and costs specification for the co-located road and pipe

To illustrate the proposed methodology and evaluate its performance in a realistic context, we consider the typical application scenario of the co-located road and pipe with flexible asphalt pavement for the road and the ductile iron for the pipe. To characterize the degradation of the road, the real field degradation performance data collected by the Florida Department of Transportation

(FDOT) are utilized. IRI is selected as the field degradation performance in this study since it is often adopted in practice for road maintenance and management. Perfect maintenance (i.e., reconstruction) will be considered when IRI exceeds a certain threshold. In this study, we will use 180 in./mile as the failure threshold. To characterize the corrosion-induced degradation of the pipe, we adopt the pipe corrosion prediction model introduced by Li et al. [30]. In [30], a Gamma process was employed to characterize the stochastic corrosion process of the ductile iron pipe with the shape parameter function of $\alpha(t) = 0.2t^{0.8}$ and the scale parameter of $\phi = 2$. Based on the industrial standard [37], the chosen pipe's diameter is set as 54" and the pipe's nominal wall thickness is set as 0.79", respectively, in this study. When the corroded depth exceeds pipe's wall thickness, a water break will be triggered due to the corrosion-induced failure mode. For illustration purposes without losing generality, we further assume the length of the co-located section as 200 feet with a standard lane width of road as 12 feet. Table 1 below summarizes all the aforementioned setting for the case study.

Table 1: Numerical settings of model parameters

Descriptions of model parameters and variables	Specified values
Shape function $\alpha(t) = ct^v$ of the Gamma process	$c = 0.2$
	$v = 0.8$
Scale parameter ϕ of the Gamma process	$\phi = 2$
Failure threshold for road degradation	180 in./mile
Pipe diameter	54"
Pipe nominal wall thickness	0.79"
Co-located section length	200'
Road standard lane width	12'

The degradation performance of both road and pipe are further discretized into a finite number of condition states. For illustration purposes, five condition states are also considered for both road and pipe, i.e., $s_t^{\mathrm{R}} \in \mathbf{S}^{\mathrm{R}}, s_t^{\mathrm{P}} \in \mathbf{S}^{\mathrm{P}}$, and $\mathbf{S}^{\mathrm{R}} = \mathbf{S}^{\mathrm{P}} = \{1, 2, 3, 4, 5\}$. Table 2 summarizes the discretized states as well as the associated cutting points for both road and pipe. For the road, the discretization is based on the typical IRI thresholds suggested in industrial practice for road maintenance and rehabilitation [1]. For the pipe, the thresholds are often considered differently in practice by water utilities based on their domain knowledge of expertise [38]. For illustration purposes without losing generality, we evenly divide the wall thickness of pipe into five categories. For the co-located road and pipe pair, there are 25 combinations of these states. As described in Eq. (10), the joint state will be denoted as a two-dimensional vector, i.e., $\boldsymbol{s}_t = \left(s_t^{\mathrm{R}}, s_t^{\mathrm{P}}\right)$. For example, a joint state $\boldsymbol{s}_t = (3,\ 4)$ indicates that at current time t, the road is at condition state $s_t^{\mathrm{R}} = 3$ and the pipe is at condition state $s_t^{\mathrm{P}} = 4$, respectively. Three maintenance actions, namely "DN", "MM", "PM", are considered for both the road and pipe. For the co-located road and pipe pair, there are 9 combinations of maintenance actions, and thus,

a joint maintenance action vector $\boldsymbol{a}_t$ is further introduced, i.e., $\boldsymbol{a}_t = \left(a_t^{\mathrm{R}}, a_t^{\mathrm{P}}\right)$. For example, a joint action $\boldsymbol{a}_t$ =(MM, PM) indicates that the road and pipe maintenance actions at current time t are a_t^{R} = MM and a_t^{P} = PM, respectively. Realistic cost information, such as road maintenance costs, pipe maintenance costs as well as user costs are further specified to the cost parameters in Section 2.2, based on the existing literature [35, 39, 40], are summarized in Table 3. The overall planning horizon is specified as 5 years.

Table 2: Discretized states and the cutting points for road (left) and pipe (right).

s_t^{R}	IRI value (in./mile)	s_t^{P}	Corroded depth (in.)
1	IRI ≤ 60	1	$0 \leq D(t) \leq 0.158$
2	$60 <$ IRI ≤ 95	2	$0.158 < D(t) \leq 0.316$
3	$95 <$ IRI ≤ 120	3	$0.316 < D(t) \leq 0.474$
4	$120 <$ IRI ≤ 180	4	$0.474 < D(t) \leq 0.632$
5	$180 <$ IRI	5	$0.632 < D(t) \leq 0.79$

Table 3: Cost information summary of the case study.

Type of cost	Condition states				
	State 1	State 2	State 3	State 4	State 5
Cost structure of road					
$C_{\mathrm{insp}}^{\mathrm{R}}$ (\$)	500				
C_{m} for $a_t^{\mathrm{R}} =$ MM (\$)	8,000				
C_{m} for $a_t^{\mathrm{R}} =$ PM (\$)		38,196	58,374	81,458	109,977
C_{tc} for $a_t^{\mathrm{R}} =$ MM	\$1,200/day				
C_{tc} for $a_t^{\mathrm{R}} =$ PM (\$)	10% of $C_{\mathrm{m}}(s_t^{\mathrm{R}}, a_t^{\mathrm{R}} = \mathrm{PM})$				
C_{u} (\$)	40,528	57,160	81,655	122,483	204,138
$C_{\mathrm{u_{maint}}}^{\mathrm{R}}$ for $a_t^{\mathrm{R}} =$ MM	\$2,946/day				
$C_{\mathrm{u_{maint}}}^{\mathrm{R}}$ for $a_t^{\mathrm{R}} =$ PM	\$5,158/day				
Cost structure of pipe					
$C_{\mathrm{insp}}^{\mathrm{P}}$ (\$)	500				
C_{m} for $a_t^{\mathrm{P}} =$ MM (\$)	7,273				
C_{m} for $a_t^{\mathrm{P}} =$ PM (\$)	47,346				
Cr (\$)	3,546				
C_{u} (\$)	0	3,637	7,273	14,547	236,730
$C_{\mathrm{u_{prop}}}^{\mathrm{P}}$	\$2,946/day				

3.1.2. Traffic load effect evaluation

In addition to the corrosion-induced pipe failure, there is also a competing failure mode of TLI failure for the pipe due to the influence of traffic load exerted on the co-locate road. Based on the current condition of the pipe, the traffic load may affect the underneath pipe differently. An old pipe with poorer condition tends to be more vulnerable to the traffic load propagated from the

road than a brand-new pipe. In addition, the different depths of cover (the distance from the surface to the top of the buried pipe) may also lead to the different effects of traffic load on the risk of pipe break. Under a good design scenario, the depth of cover will be designed to satisfy some minimum regulation parameters. However, in a bad design scenario when the pipe is placed closer to the surface of road than the designed regulations, or when defects (resulting from the road installation) or sinkholes exist in the soil, the depth of cover will be concisely smaller, making the pipe more vulnerable to the traffic load and the overall failure risk will increase. To explicitly evaluate the traffic-load effect from the road to its underneath pipe under different depth of cover scenarios, FEA is considered. Specifically, in this study, the diameter of the pipe is set as 54" and the regulation for the minimum depth of cover is set as 48" [41]. The depth of cover is then discretized into three conditions, namely good design (with "depth of cover" $\geq$ 48"), bad design (with 48" > "depth of cover" $\geq$ 38") and very bad design (with 38" > "depth of cover" $\geq$ 0").

To further represent random traffic environment, we consider the traffic load distribution in [42] with vehicle classes I, II, III and IV and their associated probabilities 0.883, 0.037, 0.074, and 0.006, respectively. For each class, its total weight from the regulation is used as the input for the FEA. The vehicle class settings are summarized in Table 4. Each pipe material has its yield strength measured in psi unit. If the stress on the material exceeds its yield strength value, it indicates a structural failure in the material. Ductile iron is used as the pipe material in this study and the designed yield strength of ductile iron pipe is set as 40,000 psi. As abovementioned, FEA implementation is carried by using software ANSYS [34]. Based on the FEA results, the traffic load has no effect on the pipe when the pipe is in good to fair condition (i.e., $s_t^{\mathrm{P}} = 1, 2, 3$). However, the impact of traffic load on pipe can be clearly seen when the pipe is in worsened condition (i.e., $s_t^{\mathrm{P}} = 4$). Table 4 also summarizes the FEA results representing the impact of different vehicle classes on the pipe at state "4". The "1" (or "0") status indicates whether TLI failure has been triggered (or not). The TLI failure probabilities of pipe under different corrosion states and depth scenarios are summarized in Table 5. The TLI failure mode is further integrated with the corrosion-induced failure mode, as discussed in Section 2.1.3, to capture the degradation of the pipe with physical dependence from the co-located road.

3.2. Performance comparison

To demonstrate the effectiveness of the proposed maintenance strategy and emphasize the benefits of considering interdependency as well as performing joint maintenance decision-making, we will compare it with several existing maintenance strategies as benchmarks, namely S1 and S2. These alternative maintenance strategies mainly maintain the road or pipe separately without considering their interdependencies [38, 43, 44]. In the first maintenance strategy (S1), road maintenance decisions, i.e., $\pi_{\mathrm{I}}^{\mathrm{R}*}\left(s_t^{\mathrm{R}}\right)$, will be determined in a proactive manner by minimizing the long-term cost of road as follows:

Table 4: Vehicle class settings and FEA results when $s_t^{\mathrm{P}} = 4$.

Vehicle class	Numbers of axles	Axle load (lb)	Good design	Bad design	Very bad design
Class I	2 axles	4000-4000 (steering-single)	0	0	0
Class II	2 axles	22000-22000 (steering-single)	0	1	1
Class III	4 axles	10000-40000-22000 (steering-tandem-single)	1	1	1
Class IV	6 axles	10000-30000-40000 (steering-tandem-tridem)	1	1	1

Table 5: TLI failure probabilities of pipe under different scenarios.

Type of design	p_{d_1}	p_{d_2}	p_{d_3}	p_{d_4}
Good	0	0	0	0.08
Bad	0	0	0	0.12
Very bad	0	0	0	0.12

$$\pi_{\mathrm{I}}^{\mathrm{R}*}\big(s_t^{\mathrm{R}}\big) = \underset{a_t^{\mathrm{R}} \in \mathbf{A}^{\mathrm{R}}}{\arg\min}\{C_{\mathrm{insp}}^{\mathrm{R}} + C_{\mathrm{m}}\big(s_t^{\mathrm{R}}, a_t^{\mathrm{R}}\big) + C_{\mathrm{tc}}\big(a_t^{\mathrm{R}}\big) + C_{\mathrm{u}}\big(s_t^{\mathrm{R}}, a_t^{\mathrm{R}}\big) + \sum_{s_{t+1}^{\mathrm{R}} \in \mathbf{S}^{\mathrm{R}}} \Pr\big(s_{t+1}^{\mathrm{R}} | s_t^{\mathrm{R}}, a_t^{\mathrm{R}}\big) \times \gamma \times V_{\pi^{\mathrm{R}}}\big(s_{t+1}^{\mathrm{R}}\big)\} \tag{21}$$

On the other hand, the pipe maintenance decisions, i.e., $\pi_{\mathrm{I}}^{\mathrm{P}*}\big(s_t^{\mathrm{P}}\big)$, will be determined in a reactive manner based on the following rule-based strategies:

$$\pi_{\mathrm{I}}^{\mathrm{P}*}\big(s_t^{\mathrm{P}}\big) = \begin{cases} a_t^{\mathrm{P}} = \mathrm{DN} \text{ if } s_t^{\mathrm{P}} \in \mathbf{S}^{\mathrm{P}} \backslash \{\mathrm{N}^{\mathrm{P}}\} \\ a_t^{\mathrm{P}} = \mathrm{PM} \text{ if } s_t^{\mathrm{P}} = \mathrm{N}^{\mathrm{P}} \end{cases} \tag{22}$$

As shown in Eq. (22), pipe will be only repaired perfectly once there is a complete failure of the pipe (i.e., pipe breaks) observed. In the second maintenance strategy (S2), both the road and pipe will be repaired in a proactive manner. The road maintenance decision, i.e., $\pi_{\mathrm{I}}^{\mathrm{R}*}\big(s_t^{\mathrm{R}}\big)$, will be determined based on Eq. (21). Similarly, the pipe maintenance decision, i.e., $\pi_{\mathrm{II}}^{\mathrm{P}'*}\big(s_t^{\mathrm{P}}\big)$, will be determined by minimizing the long-term cost written as follows.

$$\pi_{\mathrm{II}}^{\mathrm{P}'*}\big(s_t^{\mathrm{P}}\big) = \underset{a_t^{\mathrm{P}} \in \mathbf{A}^{\mathrm{P}}}{\arg\min}\{C_{\mathrm{insp}}^{\mathrm{P}} + C_{\mathrm{m}}\big(s_t^{\mathrm{P}}, a_t^{\mathrm{P}}\big) + C_{\mathrm{tc}}\big(a_t^{\mathrm{P}}\big) + C_{\mathrm{u}}\big(s_t^{\mathrm{P}}, a_t^{\mathrm{P}}\big) + \sum_{s_{t+1}^{\mathrm{P}} \in \mathbf{S}^{\mathrm{P}}} \Pr\big(s_{t+1}^{\mathrm{P}} | s_t^{\mathrm{P}}, a_t^{\mathrm{P}}\big) \times \gamma \times V_{\pi^{\mathrm{P}}}(s_{t+1}^{\mathrm{P}}) \}} \tag{23}$$

To compare the proposed and alternative maintenance strategies (i.e., S1 and S2), they are evaluated on the same road and pipe characteristics as well as cost information described in Section 3.1.1. In addition, since the proposed maintenance strategy considers the interdependencies between road and pipe, the propagated effect from pipe to road is set as $\beta = 2$ and the traffic-load effect from road to pipe is determined with $p_{\mathrm{d}_4} = 0.08$ The influence of these dependence parameters on maintenance decisions will be comprehensively investigated in the next section.

Fig. 4(a) shows the comparison between the expected total cost of the proposed strategy and alternative strategies over the 5-year planning period. As shown in the figure, the proposed work considered both joint and proactive maintenance of the co-located road and pipe with interdependencies exhibits the same or lower cost than alternative strategies under different conditions of the road and pipe. In particular, when the pipe is in a worse condition (e.g., state 4), more cost saving can be achieved. In addition, the figure shows that proactive maintenance in both the proposed strategy and S2 will be beneficial in terms of reducing the total cost as compared to the rule-based reactive maintenance strategy in S1 when there exists certain degradation of the pipe (e.g., states $2-4$). The total cost consists of both the costs of maintenance related activities (i.e., maintenance, traffic control, and inspection) and the user costs (i.e., long-term and short-term costs).

To further explain why the proposed work can achieve the overall cost reduction, Figs. 4(b) and 4(c) show the corresponding expected maintenance costs and user costs of the proposed work over existing maintenance strategies under different conditions of the co-located road and pipe. As shown in these figures, when the pipe is deteriorating with certain degradation conditions (e.g., states $2-4$), both the proposed and S2 maintenance strategies tend to initiate more proactive maintenance for pipe as compared to S1 when maintenance strategy is only triggered if the pipe is completely failed. Such additional maintenance costs for proactive maintenance will be translated to significant cost reduction from the user costs perspective, as shown in Fig. 4(c). In addition, when the pipe becomes more deteriorated (e.g., state 4), the proposed work tends to allocate more maintenance efforts for the pipe due to its anticipation of negative consequences of pipe breaks on its co-located road. Such maintenance efforts further translate to user costs reduction as well as the overall cost reduction as compared to S2.

After comparing the performance between the proposed maintenance strategy and alternative strategies, we further investigate and compare the difference of optimal maintenance actions obtained under different strategies and Fig. 5 graphically summarizes the comparison results. Since the maintenance planning period is assumed as five years, five action pairs of each joint state pair during this five-year period are shown horizontally. The coded colors for the maintenance actions are black for "PM", gray for "MM", and light gray for "DN". Ideally, there are 25 joint states in total. For illustration simplicity, we only demonstrate the states associated with different maintenance actions obtained under different strategies in Fig. 5. For the condition states which

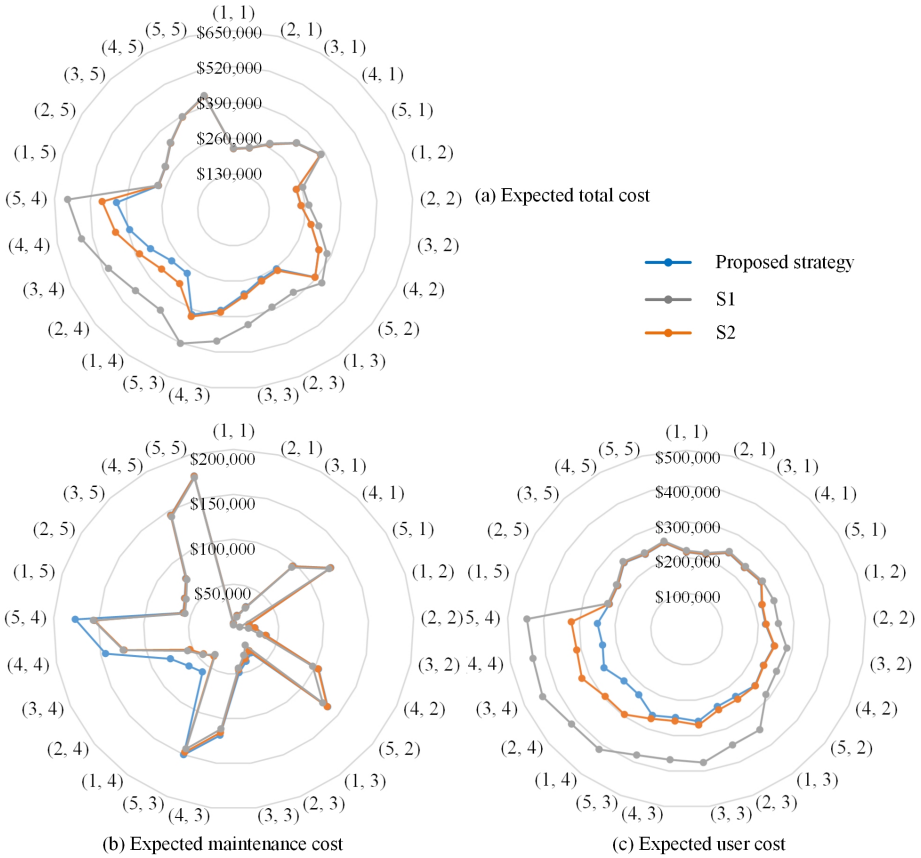

Figure 4: Performance comparison between the proposed and alternative maintenance strategies.

have the same maintenance actions among different strategies throughout the five-year time period, they are omitted. The complete proposed maintenance policy for all the combinations of states can be found in Appendix B. For those condition states which have the same maintenance actions on specific years, the corresponding maintenance actions are donated as "-". Fig. 5 results can serve as a lookup table to inform the maintenance policies for the road and pipe maintenance stakeholders. Specifically, based on the joint condition states of a co-located road and pipe at the beginning of each year, the corresponding maintenance actions (suggested under different strategies) can be obtained. Take a co-located road and pipe with condition states of (4, 4) at the beginning of year 1 (i.e., current planning time) as an example, the proposed work suggests considering "PM" at the beginning of year 1. After restoring them into perfect conditions, the co-located pair will experience a whole year (e.g., from year 1 to year 2) of degradation and may end up at any combination of joint condition

states with varied probabilities. At the beginning of year 2, based on the actual condition states, the stakeholders can refer to the corresponding suggested maintenance actions. But since "PM" is adopted at year 1, the co-located pair with have a close-to-one probability of having good conditions at the beginning of year 2. The stakeholders will more likely to adopt decisions suggested at the top rows of the lookup table in practice. But the lookup table essentially enumerates all the possible scenarios although some of them may be in very low probabilities) and provides the corresponding suggested decisions.

As shown in Figs. 5(a) and 5(b), the proposed strategy has a darker color of maintenance actions in general than strategies S1 and S2. This indicates that the proposed strategy tends to recommend a higher level of pipe maintenance activities for the same joint condition state than alternative strategies, even when the co-located road and pipe exhibit conflicting degradation states. For example, in the first year, the joint state $(1, 4)$ is recommended to have action pair (DN, PM) in the proposed strategy, but (DN, DN) in S1 and (DN, MM) in S2. The proposed strategy recommends higher-level maintenance action of performing "perfect maintenance" for the pipe than "do nothing" in S1 and "minor maintenance" in S2. There are multiple reasons to explain this finding. First, by taking into account the dependency from road to pipe (i.e., traffic-load effect) in the proposed work, the long-term user costs for the pipe will be increased since pipe is more likely to fail. To anticipate such increased failure risk from the pipe, more proactive maintenance actions tend to be initiated. Second, since the joint road and pipe maintenance will avoid the repaving costs of co-located areas as well as reduce the traffic control costs, the maintenance costs under the same level of maintenance activities will be reduced. Therefore, given the same maintenance budget, it becomes more affordable for the proposed strategy to consider a higher-level maintenance action.

To further clarify why the proposed maintenance strategy has better cost performance while proposing a higher level maintenance activities, take state $\boldsymbol{s}_t = (2, 2)$ which is recommended to have action $a_t =$(MM, MM) on the first year as another example. First, while doing joint maintenance, the maintenance costs of road and pipe based on the proposed approach becomes $C^{\mathrm{R}}_{\mathrm{insp}} + C^{\mathrm{P}}_{\mathrm{insp}} + C_{\mathrm{m}}\big(s^{\mathrm{R}}_t = 2, a^{\mathrm{R}}_t = \mathrm{MM}\big) + C_{\mathrm{m}}\big(s^{\mathrm{P}}_t = 2, a^{\mathrm{P}}_t = \mathrm{MM}\big) - \mathrm{I}_{\left\{a^{\mathrm{R}}_t = \mathrm{MM} \neq \mathrm{DN} \ \&\ a^{\mathrm{P}}_t = \mathrm{MM} \neq \mathrm{DN}\right\}} \times Cr + \max\big(C_{\mathrm{tc}}\big(a^{\mathrm{R}}_t = \mathrm{MM}\big), C_{\mathrm{tc}}\big(a^{\mathrm{P}}_t = \mathrm{MM}\big)\big) = \$13,927$. However, if the road and pipe maintenance activities are performed separately in alternative strategies (i.e., S1 and S2), the total maintenance cost will be calculated as $C^{\mathrm{R}}_{\mathrm{insp}} + C^{\mathrm{P}}_{\mathrm{insp}} + C_{\mathrm{m}}\big(s^{\mathrm{R}}_t = 2, a^{\mathrm{R}}_t = \mathrm{MM}\big) + C_{\mathrm{m}}\big(s^{\mathrm{P}}_t = 2, a^{\mathrm{P}}_t = \mathrm{MM}\big) + C_{\mathrm{tc}}\big(a^{\mathrm{R}}_t = \mathrm{MM}\big) + C_{\mathrm{tc}}\big(a^{\mathrm{P}}_t = \mathrm{MM}\big) = \$18,473$. This shows that for the same type of maintenance actions, the proposed strategy tends to be more affordable than alternative ones. In other words, if maintenance budget is allowed, maintenance actions with higher-level of repair efforts will be more likely to be considered in the proposed strategy. Further, under this scenario of $\boldsymbol{s}_t = (2, 2)$ with action $\boldsymbol{a}_t =$(MM, MM), the joint maintenance based on the proposed strategy will finish the maintenance activity more efficiently with road blockage reduced one day, which will be further translated to the reduction of short-term user

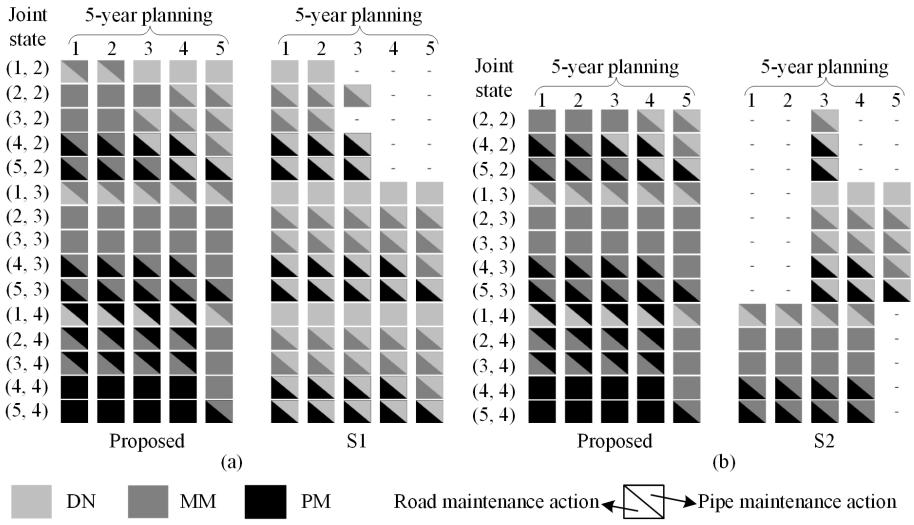

Figure 5: Comparison of maintenance policies between (a) the proposed strategy and S1; (b) the proposed strategy and S2.

costs for the road as well. Specifically, the actual short-term user costs by the proposed approach can be calculated as $C^{\mathrm{R}}_{\mathrm{u_{maint}}}\left(s^{\mathrm{R}}_t = 2, a^{\mathrm{R}}_t = \mathrm{MM}\right) \times T^{\mathrm{R}} + (\beta - 1) \times C^{\mathrm{P}}_{\mathrm{u_{prop}}}\left(s^{\mathrm{P}}_t = 2, a^{\mathrm{P}}_t = \mathrm{MM}\right) \times T^{\mathrm{P}} = \$5,892$. Meanwhile, by using the alternative strategies of separate maintenance (i.e., S1 and S2), the total traffic blockage for two maintenance activities are two days, and the actual cost is $C^{\mathrm{R}}_{\mathrm{u_{maint}}}\left(s^{\mathrm{R}}_t = 2, a^{R}_t = \mathrm{MM}\right) \times T^{\mathrm{R}} + \beta \times C^{\mathrm{P}}_{\mathrm{u_{prop}}}\left(s^{\mathrm{P}}_t = 2, a^{\mathrm{P}}_t = \mathrm{MM}\right) \times T^{\mathrm{P}} = \$8,838$. This explains the potential user costs reduction achieved by the proposed joint maintenance strategy over alternative strategies.

Another general pattern displayed in Fig. 5 is that when the condition state of pipe becomes worsened, the proposed strategy tends to consider higher-level of maintenance activities more frequently over existing strategies of S1 and S2. For instance, as shown in Fig. 5(b), when pipe is at condition state "2", the proposed strategy only plans a higher-level of maintenance activity on year 3 as compared to S2. When the condition state of the pipe deteriorates, e.g., state "4", the proposed strategy plans to consider higher-level of maintenance activities from years 1 to 4. Such more frequent adjustment of the maintenance activities in a more proactive manner essentially aims to reduce the negative influence of complete failure (i.e., state "5") of the pipe, such as the increase of pipe and road user costs due to pipe breaks. It further confirms the results shown in Fig. 4 that when the pipe is at worsened condition state, the maintenance costs of the proposed strategy tend to be higher than the conventional strategies (i.e., S1 and S2). However, such maintenance efforts are beneficial to the reduction of users costs and the total cost.

3.3. The impact from road and pipe interdependencies to maintenance decisions

In section 3.2, the propagated effect of pipe activities on road users, and the traffic-load effect from road to TLI failure mode of the pipe are both specified at medium levels, i.e., $\beta = 2, p_{\mathrm{d}_4} = 0.08$ It is still unclear how each factor will influence the cost performance as well as the maintenance actions under different maintenance strategies. This section will provide sensitivity analysis by investigating the marginal effect of each factor on maintenance decisions under different maintenance strategies.

3.3.1. Influence of propagated effect

The propagated effect parameter β, as shown described in section 2.2 and Fig. 3, represents the impact of pipe maintenance activity on the co-located roads and such impact may vary depending on the number of co-located road sections affected. In this section, a sensitivity analysis will be performed by considering three scenarios of β, namely $\beta = 1$, 2, and 4. They represent scenarios of pipe maintenance activity affecting one, two, and four road sections (including the co-located road section under repair as well as its neighboring road sections), respectively. The traffic-load effect parameter, denoted by p_{d_i}, is assumed to be fixed as 0.08 when pipe condition state is "4", i.e., $p_{\mathrm{d}_4} = 0.08$

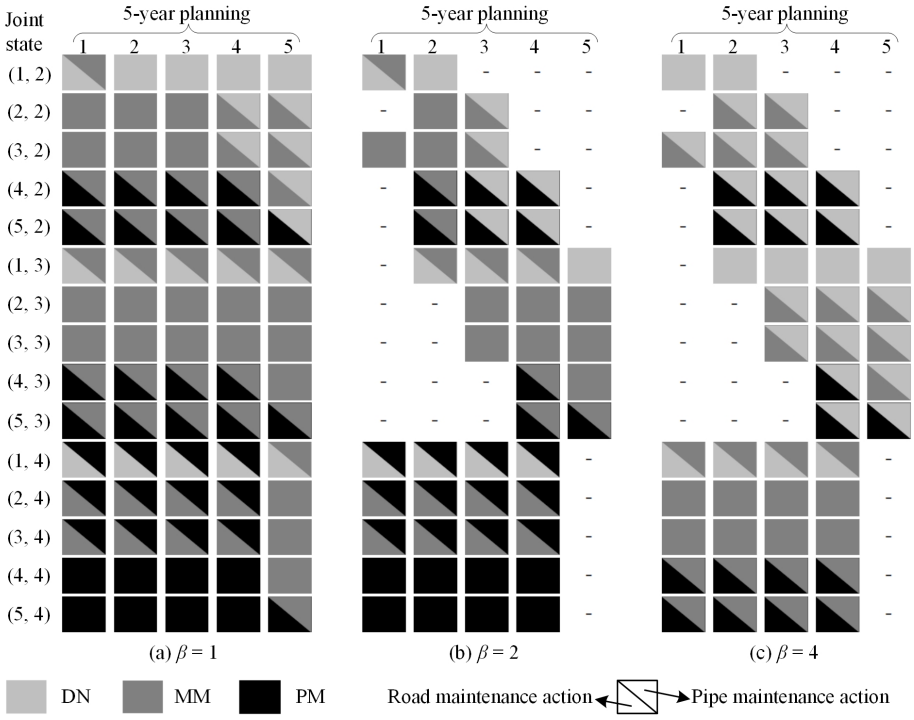

Figure 6: The comparison of optimal maintenance actions under different propagated effect scenarios.

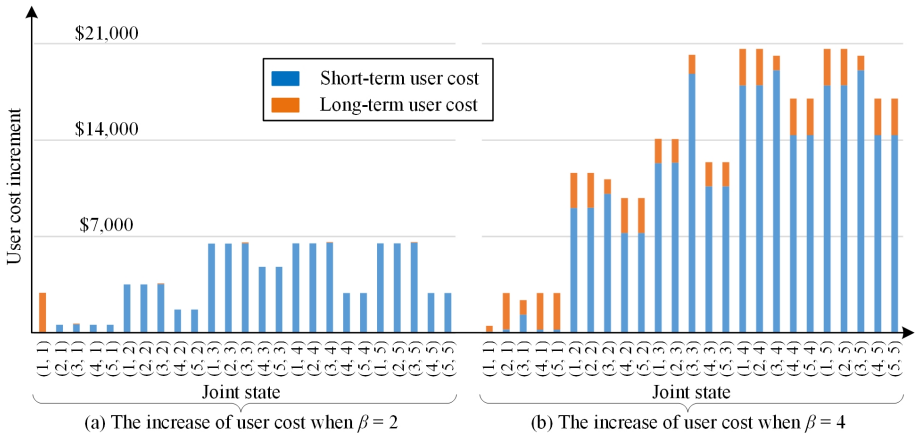

Figure 7: The user costs increment of $\beta = 2$ (a) and 4 (b) and baseline scenario of $\beta = 1$.

We first investigate how the propagated effect parameter will influence the maintenance decisions under the proposed maintenance strategy. Fig. 6 shows the comparison results of optimal maintenance actions obtained under different β values. As shown in the figure, when the propagated effect increases, the proposed maintenance strategy tends to consider a lower-level maintenance activity. Taking the joint state of $(1, 2)$ as an example, the optimal maintenance actions for the pipe in the first 2 years are (MM, MM), (MM, DN) and (DN, DN), under $\beta = 1, 2, 4$, respectively. It can be explained as follows. Based on Eqs. (13) and (16), the value of β directly affects the short-term user costs. The higher value of propagated effect means that more traffic blockage will be involved when the maintenance is performed on the pipe. To minimize the overall maintenance costs, including both the short-term and long-term user costs, good maintenance actions need to balance well between triggering high-level maintenance activities (to minimize the long-term user coasts in a proactive manner) and adopting lower-level ones (to reduce the disruption of pipe maintenance on road sections due to traffic blockage). Fig. 7 shows the short-term and long-term user costs increment under scenarios of $\beta = 2$ and 4 by using $\beta = 1$ as the baseline scenario. As shown in the figure, when β value increases, it is associated with larger short-term user costs increment (in blue) over long-term user costs increment (in orange). Thus, since the increment of short-term user costs dominates when β increases, the proposed maintenance strategy tends to recommend less aggressive maintenance activities to mitigate the short-term user costs increment and ensure the overall cost reduction. It is noticed that when the pipe is at failure state, i.e., $s_t^{\mathrm{R}} = 5$, its failure not only impacts water users, but also the co-located road and its neighboring roads. The failure cost of the failed pipe and potential cascading costs due to road failure can be tremendous if the pipe is not replaced. Thus, the following rule-based constraint is embedded in the proposed optimization model. That is, the pipe will be always repaired when it is in a failure state (i.e., $s_t^{\mathrm{R}} = 5$) regardless of how many road

sections will be negatively affected. This can be reflected in the results of joint states scenarios with $s_t^{\mathrm{R}} = 5$ in Appendix B. Noticed that for visualization simplicity, Fig. 6 only shows the results of states when there are differences among maintenance actions under different β values. For those omitted state pairs, the maintenance actions under different β values are the same, which can be found in the complete maintenance results in Appendix B.

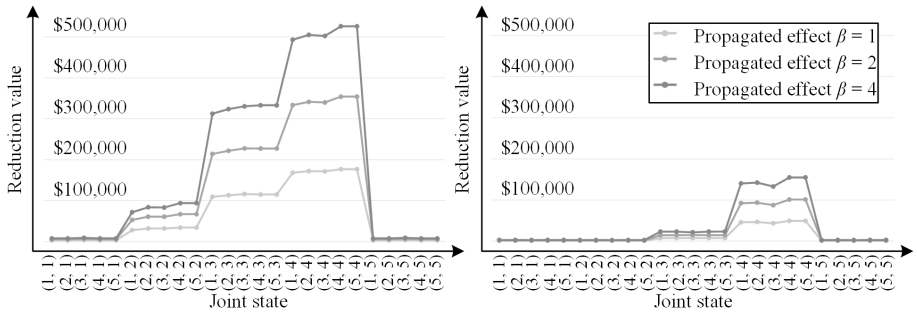

(a) Proposed vs. S1 (b) Proposed vs. S2

Figure 8: The influence of propagated effect on total cost reduction achieved by the proposed strategy over (a) S1 and (b) S2.

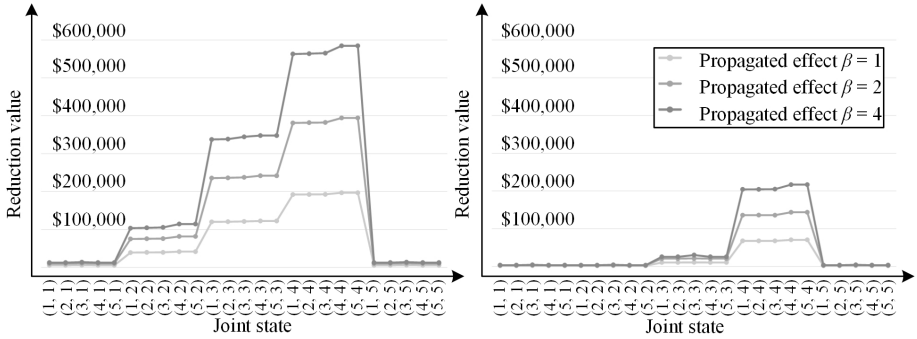

(a) Proposed vs. S1 (b) Proposed vs. S2

Figure 9: The influence of propagated effect on user costs reduction achieved by the proposed strategy over (a) S1 and (b) S2.

We further investigate the cost reduction achieved by the propped strategy over existing strategies of S1 and S2 under different scenarios of propagated effect. Figs. 8 and 9 compare the overall cost reduction as well as the user costs reduction between the proposed and alternative strategies under $\beta = 1, 2,$ and 4. As shown in Figs. 8 and 9, the proposed maintenance strategy will exhibit more significant cost reduction when the pipe is at worsened condition states. As discussed in Section 3.2, such overall cost reduction is essential due to the reduction of user costs since more proactive maintenance activities are recommended in the proposed strategy. In addition, as β increases, both the overall cost reduction

and user costs reduction will increase as well. It is due to the fact that a higher value of β is associated with a higher impact of pipe failure to its co-located road sections. By considering such operational dependency and providing more proactive maintenance to avoid complete failure of the pipe, the proposed work is able to mitigate the short-term user costs increase resulting from the increased traffic blockage and ultimately achieve the overall cost reduction.

3.3.2. Influence of traffic-load effect

After investigating the marginal effect of propagated effect on pipe to road, we further investigate the influence of traffic-load effect from road to pipe, captured by the induced probability p_{d_i}. Based on the results from the FEA model shown in Section 3.1.2, the traffic-load effect has the highest impact on the pipe when pipe is in corrosion state "4", i.e., $p_{\mathrm{d}_1} = p_{\mathrm{d}_2} = p_{\mathrm{d}_3} = 0$. Therefore, by fixing $\beta = 2$, we perform the sensitivity analysis of traffic-load effect under three scenarios, namely $0, 0.08$, and 0.12, when the state of the pipe is "4". They represent scenarios of traffic having negligible, minor, and moderated acceleration on pipe degradation and TLI failure risk.

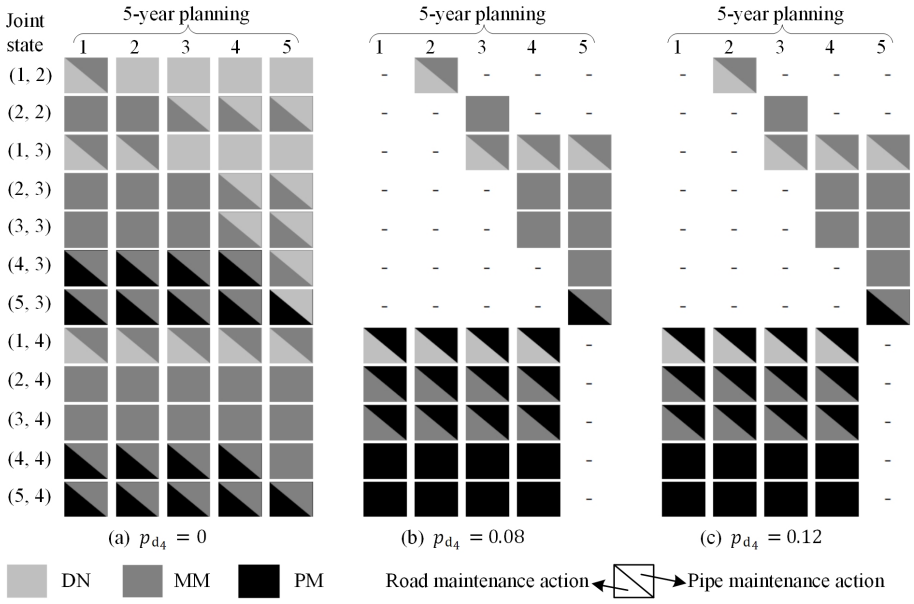

Figure 10: The influence of traffic-load effect on maintenance policy.

Similar to Section 3.3.1, we begin with investigating the influence of traffic-load effect on optimal maintenance decision of the proposed strategy. Fig. 10 shows the comparison results of optimal maintenance actions obtained under different traffic-load effect. The full maintenance policy can be found in Appendix B. As shown in Fig. 10, compared to the scenario of negligible traffic-load effect, the proposed strategy tends to suggest a higher level of maintenance activities

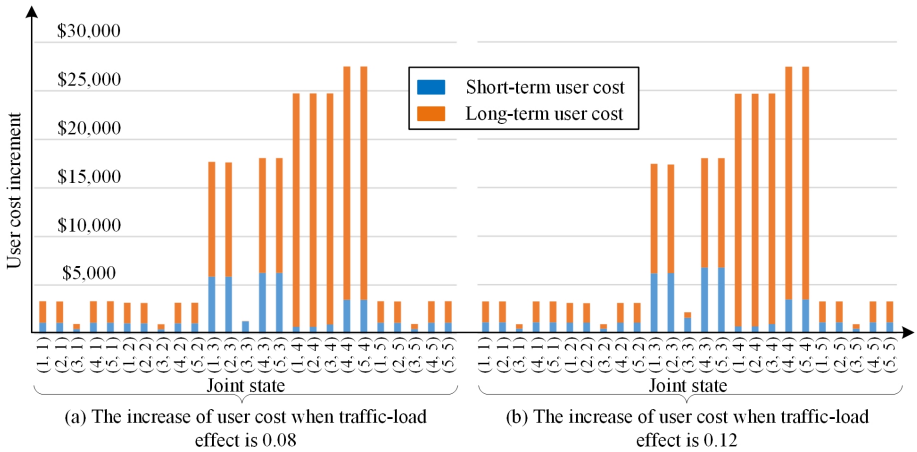

(a) The increase of user cost when traffic-load effect is 0.08

(b) The increase of user cost when traffic-load effect is 0.12

Figure 11: The influence of traffic-load effect on user costs increment.

when there is significant traffic-load effect. Take joint state $(5, 3)$ as an example, when $p_{\mathrm{d}_4} = 0$, the proposed strategy recommends "DN" for the pipe. When p_{d_4} increases to 0.08 or 0.12, the pipe is recommended to have "MM". It is because when traffic-load effect becomes more significant, the pipe has more tendency to fail, which leads to an increase in long-term user costs if more conservative maintenance activities are considered. To further demonstrate this, Fig. 11 shows the long-term and short-term user costs increment under scenarios of $p_{d_4} = 0.08$ and 0.12 by using $p_{\mathrm{d}_4} = 0$ as the baseline scenario. It shows that when traffic-load effect becomes significant, the larger increment of long-term user cost increment (in orange) is involved than that of the short-term user costs (in blue). Thus, to minimize the overall user costs as well as total cost, the proposed strategy tends to suggest higher-level maintenance activities.

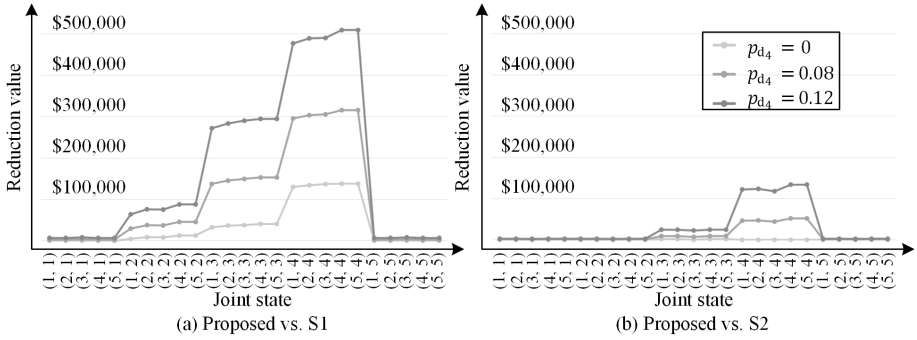

(a) Proposed vs. S1

(b) Proposed vs. S2

Figure 12: The influence of traffic-load effect on total cost reduction achieved by the proposed strategy over (a) S1 and (b) S2.

We further investigated the overall cost reduction (in Fig. 12) and user

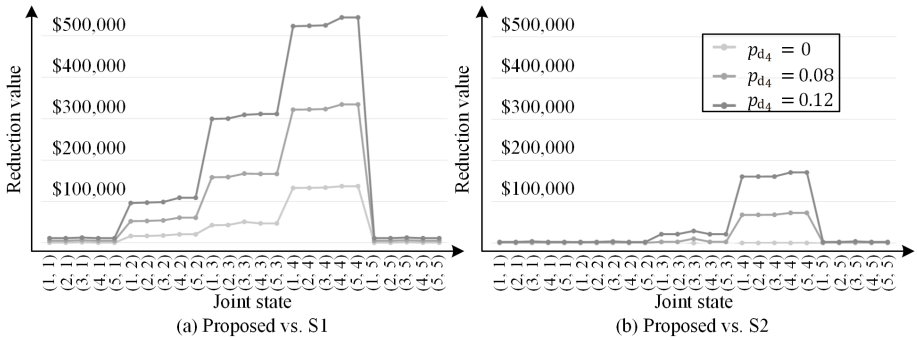

Figure 13: The influence of traffic-load effect on user costs reduction achieved by the proposed strategy over (a) S1 and (b) S2.

costs reduction (in Fig. 13) of the proposed maintenance strategy over S1 and S2 under different scenarios of traffic-load effect. As shown in both figures, the proposed exhibit more significant cost reduction at worsened conditions of the pipe. In addition, as the traffic-load effect becomes more significant, the associate cost reduction of the proposed strategy over alternative strategies will increase as well. This is due to the fact that by taking into account such failure dependence from road to pipe, the proposed work is able to provide a more proactive maintenance strategy to mitigate the long-term user costs increase resulting from an increased pipe failure risk and ultimately achieve the overall cost reduction.

4. Conclusion

In this paper, a joint long-term proactive maintenance planning framework has been proposed for the co-located road and pipe by explicitly accounting for their complex interdependencies, including both the physical dependency from road to pipe and the operational dependency from pipe to road. To capture the influence of traffic load effect on the pipe failure probability, finite element modeling is first established to comprehensively evaluate the TLI sudden failure mode of the pipe under varied traffic conditions and road design scenarios, and a probabilistic model is further formulated to simultaneously take into account the competing risk of both the TLI sudden failure mode as well as corrosion-induced gradual failure mode of the pipe. Then a joint maintenance planning model is established by taking into account the operational dependency from pipe to road under different co-located scenarios to minimize the overall costs, including the maintenance costs, short-term user costs and long-term user costs of both the co-located road and pipe.

As demonstrated in the case study, the proposed proactive maintenance strategy exhibits more cost-saving benefits as compared to several existing maintenance planning strategies which consider road and pipe maintenance separately, such as S1 of proactive maintenance of road and reactive maintenance

of pipe, and S2 of proactive maintenance of both the road and pipe. Such cost reduction is realized by jointly repairing the co-located road and pipe in the same time period to avoid the repaving costs due to pipe repair and decrease the overall maintenance costs by shortening traffic control time period. In addition, such cost reduction is further ensured by accurately anticipating both sudden failure mode and gradual failure mode of the pipe to initialize more aggressive maintenance activities of the pipe and avoid its negative impact on the co-located road and pipe. After demonstrating the cost-saving benefits, the influence of interdependencies on the proposed maintenance planning decisions has been also comprehensively investigated under different co-location scenarios as well as traffic load conditions. When more road sections in the neighboring area are affected by the pipe (i.e., an increase of β) and the short-term user costs become a dominant factor, the proposed method tends to generate less aggressive maintenance actions to reduce the short-term user costs due to maintenance actions. When the traffic load effect increases (e.g., an increase of p_{d_i}) and the long-term user costs become a dominant factor, the proposed method tends to generate more aggressive maintenance actions to reduce future risk of pipe breaks and reduce long-term user costs. Such marginal insights will allow stakeholders to adjust the maintenance decision of a co-located road and pipe based on their varied characteristics and traffic conditions.

For future work, we will incorporate additional physical dependency from pipe to road (e.g., leakage of the pipe potentially increasing road failure). Instead of optimizing maintenance decisions alone with a pre-determined inspection policy and assuming the ductile iron pipe, we will relax these assumptions by jointly optimizing the inspection decisions and maintenance decisions and further considering other types of pipe materials, such as polyvinyl chloride. In addition, we will extend the current work of component-level maintenance decision-making towards the next step of investigating the system-level maintenance decision-making of the co-located road and water network composed of multiple co-located pairs (i.e., components) with varied individual characteristics (e.g., degradation states, pipe length and diameter, number of traffic lanes, traffic volume, etc.). Regarding practical implementation, we will convert the developed analytical models and algorithms into a user-friendly decision-support platform and demonstrate the benefits of the proposed work to local stakeholders using showcase examples.

Acknowledgments

The authors gratefully acknowledge valuable comments of journal editors and anonymous reviewers to improve the quality and readability of the paper. This work was supported in part by National Science Foundation under Grant No. BCS-1638301, and U.S. Department of Transportation under Grant CTECH No. 69A3551747119.

Appendix A. Nomenclature

Sets and indices

$\mathbf{A}^{\mathrm{R}}, \mathbf{A}^{\mathrm{P}}, \mathbf{A}$	Sets of road, pipe and joint maintenance actions, respectively, where superscripts "R" and "P" represent "Road" and "Pipe".
$\mathbf{S}^{\mathrm{R}}, \mathbf{S}^{\mathrm{P}}, \mathbf{S}$	Set of road, pipe, and joint condition states, respectively.
$\{1, \ldots, \mathrm{T}\}$	Set of decision epochs where T is the last year of the maintenance planning horizon.

State variables

$b_1, \ldots, b_{\mathrm{N^P}}$	Cutting points of pipe discretized condition states.
$\mathrm{N}^{\mathrm{R}}, \mathrm{N}^{\mathrm{P}}$	Failure states of road and pipe, respectively.
n_i, n_{ij}	The number of road sections in state i, and the number of road sections from state i to j, respectively.
$s_t^{\mathrm{R}}, s_t^{\mathrm{P}}, \boldsymbol{s}_t$	Road, pipe, and joint condition states at time t, respectively.
x_t^{f}	Pipe sudden failure state resulting from traffic-load effect at time t, where superscript "f" represents "sudden failure".

Maintenance actions

$a_t^{\mathrm{R}}, a_t^{\mathrm{P}}, \boldsymbol{a}_t$	Road, pipe, and joint maintenance actions at time t, respectively.

Transition probabilities

$\mathbf{P}_0^{\mathrm{R}},\ p_{0_{ij}}^{\mathrm{R}}$	Road degradation transition matrix, and its composing elements, respectively.
$\mathbf{P}^{\mathrm{R}}\big(a_t^{\mathrm{R}}\big), p_{ij}^{\mathrm{R}}\big(a_t^{\mathrm{R}}\big)$	Road state transition matrix under the maintenance effect, and its composing elements, respectively.
$\mathbf{P}_0^{\mathrm{P}},\ p_{0_{ij}}^{\mathrm{P}}$	Pipe corrosion-induced transition matrix, and its composing elements, respectively.
$\mathbf{P}^{\mathrm{P}}\big(a_t^{\mathrm{P}}\big), p_{ij}^{\mathrm{P}}\big(a_t^{\mathrm{P}}\big)$	Pipe state transition matrix under maintenance effect, and its composing elements, respectively.
p_{d_i}	Probability of a pipe at condition state $i \in \mathbf{S}^{\mathrm{P}}$ suddenly fails under traffic-load effect, where subscript "d" represents traffic-load effect.
$p_{ij}^{\mathrm{f}}\big(a_t^{\mathrm{P}}\big)$	Transition probability from state i to j for a pipe given maintenance action a_t^{P} at time t under corrosion-induced and TLI.

Costs and value functions

c_1, c_2	Unit cost for delay time caused by maintenance, road condition, respectively.
c_3	Unit cost for fuel/maintaining/repairing vehicle.
$C_{\mathrm{insp}}, C_{\mathrm{insp}}^{\mathrm{R}}, C_{\mathrm{insp}}^{\mathrm{P}}$	Joint, road, and pipe inspection costs, respectively, where subscript "insp" represents "inspection".
$C_{\mathrm{m}}, C_{\mathrm{tc}}, C_{\mathrm{r}}$	Maintenance, traffic control, and repaving costs, respectively, where subscripts "m", "tc", and "r" represent "maintenance", "traffic control", and "repaving".
C_{u}	Total user costs, where subscript "'u' represents "user".
$C_{\mathrm{ust}}, C_{\mathrm{ult}}$	Short-term, and long-term user costs, respectively, where subscripts "st" and "lt" represent "short-term" and "long-term".
$C_{\mathrm{u_{maint}}}^{\mathrm{R}}, C_{\mathrm{u_{prop}}}^{\mathrm{P}}$	Road user cost caused by road, and pipe maintenance activities, respectively, where subscripts "maint" and "prop" represent "maintenance activity" and "propagated effect".

$C_{\mathrm{u}}^{\mathrm{R}}, C_{\mathrm{u}}^{\mathrm{P}}$	Vehicle owners annual costs, and water users inconvenience costs, respectively.
$D_{\mathrm{maint}}^{\mathrm{R}}$, $D_{\mathrm{maint}}^{\mathrm{P}}$	Delay time of a vehicle caused by road maintenance, pipe maintenance, respectively.
D_{opt}	Delay time of a vehicle caused by road condition, where subscript "opt" represents "operating".
$T^{\mathrm{R}}, T^{\mathrm{P}}$	Repair time of road and pipe.
TF	Traffic flow quantified by the number of vehicles per day.
T_{e}	Length of a decision epoch.
$V(\cdot)$	Value function.
π	Maintenance policy.
γ	Discount factor.
Other parameters	
$D(t), d$	Corrosion depth of pipe at time t, and its realization, respectively.
$\boldsymbol{K}, \boldsymbol{u}, \boldsymbol{F}$	Stiffness matrix, field variable vector, force vector, respectively.
β	Propagated effect.
$\boldsymbol{\theta}^{\mathrm{R}}$	Traffic-load-induced influencing factors.
$\alpha(t), c, v$	Shape function and its parameters of the Gamma process.
ϕ	Scale parameter of the Gamma process.

Appendix B. Complete maintenance actions based on the proposed strategy under the baseline settings of $\boldsymbol{\beta = 2}$ and $\boldsymbol{p_{\mathrm{d}_4} = 0.08}$.

Figs 5, 6, 10 only display the results of states when there are differences among maintenance actions under different scenarios. For those omitted state pairs, the maintenance actions under different scenarios are the same. The following table includes the omitted state pairs and shows the complete results of the proposed maintenance strategy under $\beta = 2$ and $p_{\mathrm{d}_4} = 0.08$.

References

[1] U.S. Department of Transportation - Federal Highway Administration, Length by present serviceability rating (pavement condition)/measured pavement roughness—major collectors and urban minor arterials and collectors (Report No. HM-63) (2020).

[2] S. Folkman, Water main break rates in the usa and canada: A comprehensive study, Utah State University, Buried Structures Laboratory (2018).

[3] J. Boakye, R. Guidotti, P. Gardoni, C. Murphy, The role of transportation infrastructure on the impact of natural hazards on communities, Reliability Engineering & System Safety 219 (2022) 108184. doi:10.1016/j.ress.2021.108184.

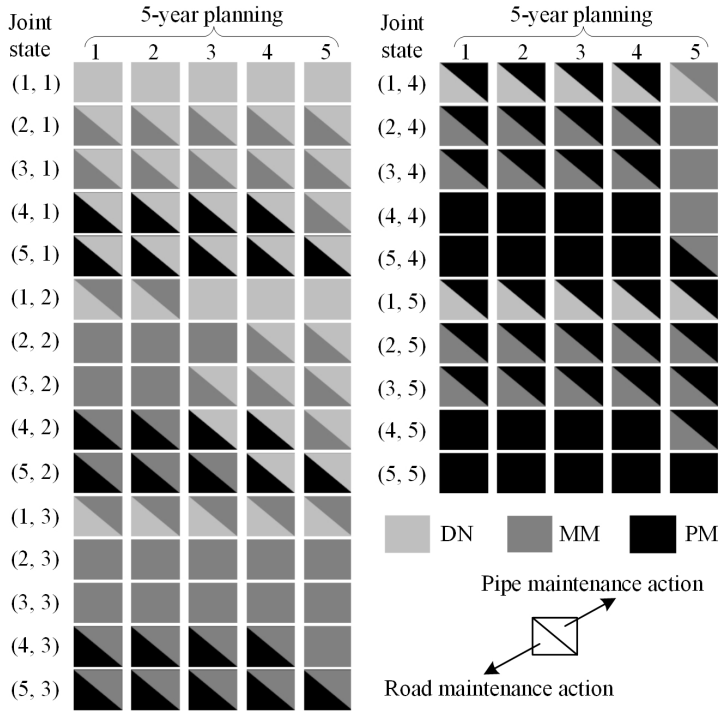

[4] M. Ouyang, Review on modeling and simulation of interdependent critical infrastructure systems, Reliability engineering & System safety 121 (2014) 43–60. doi:10.1016/j.ress.2013.06.040.

[5] P. Rajeev, J. Kodikara, D. Robert, P. Zeman, B. Rajani, Factors contributing to large diameter water pipe failure, Water asset management international 10 (3) (2014) 9–14.

[6] Z. Li, B. Zhang, Y. Wang, F. Chen, R. Taib, V. Whiffin, Y. Wang, Water pipe condition assessment: a hierarchical beta process approach for sparse incident data, Machine learning 95 (1) (2014) 11–26. doi:10.1007/s10994-013-5386-z.

[7] L. M. Jenkins, Optimizing maintenance and replacement activities for water distribution pipelines, Vanderbilt University, 2014.

[8] C. Ramos-Salgado, J. Muñuzuri, P. Aparicio-Ruiz, L. Onieva, A decision support system to design water supply and sewer pipes replacement intervention programs, Reliability Engineering & System Safety 216 (2021) 107967. doi:10.1016/j.ress.2021.107967.

[9] R. Arismendi, A. Barros, A. Grall, Piecewise deterministic markov process for condition-based maintenance models—application to critical infrastruc-

tures with discrete-state deterioration, Reliability Engineering & System Safety 212 (2021) 107540. doi:10.1016/j.ress.2021.107540.

[10] X. Zhang, H. Gao, Road maintenance optimization through a discrete-time semi-markov decision process, Reliability Engineering & System Safety 103 (2012) 110–119. doi:10.1016/j.ress.2012.03.011.

[11] S. Petchrompo, A. K. Parlikad, A review of asset management literature on multi-asset systems, Reliability Engineering & System Safety 181 (2019) 181–201. doi:10.1016/j.ress.2018.09.009.

[12] N. Sharma, P. Gardoni, Mathematical modeling of interdependent infrastructure: An object-oriented approach for generalized network-system analysis, Reliability Engineering & System Safety 217 (2022) 108042. doi:10.1016/j.ress.2021.108042.

[13] Y.-C. Yu, P. Gardoni, Predicting road blockage due to building damage following earthquakes, Reliability Engineering & System Safety 219 (2022) 108220. doi:10.1016/j.ress.2021.108220.

[14] J. Kong, C. Zhang, S. P. Simonovic, Optimizing the resilience of interdependent infrastructures to regional natural hazards with combined improvement measures, Reliability Engineering & System Safety 210 (2021) 107538. doi:10.1016/j.ress.2021.107538.

[15] N. Ghorbani-Renani, A. D. González, K. Barker, N. Morshedlou, Protection-interdiction-restoration: Tri-level optimization for enhancing interdependent network resilience, Reliability Engineering & System Safety 199 (2020) 106907. doi:10.1016/j.ress.2020.106907.

[16] M. Monsalve, J. C. de la Llera, Data-driven estimation of interdependencies and restoration of infrastructure systems, Reliability Engineering & System Safety 181 (2019) 167–180. doi:10.1016/j.ress.2018.10.005.

[17] S. Alaswad, Y. Xiang, A review on condition-based maintenance optimization models for stochastically deteriorating system, Reliability engineering & system safety 157 (2017) 54–63. doi:10.1016/j.ress.2016.08.009.

[18] Y. Chen, Y. Liu, T. Jiang, Optimal maintenance strategy for multi-state systems with single maintenance capacity and arbitrarily distributed maintenance time, Reliability Engineering & System Safety 211 (2021) 107576. doi:10.1016/j.ress.2021.107576.

[19] H. Wang, H. Liao, X. Ma, R. Bao, Remaining useful life prediction and optimal maintenance time determination for a single unit using isotonic regression and gamma process model, Reliability Engineering & System Safety 210 (2021) 107504. doi:10.1016/j.ress.2021.107504.

[20] R. Dekker, R. E. Wildeman, F. A. Van der Duyn Schouten, A review of multi-component maintenance models with economic dependence, Mathematical methods of operations research 45 (3) (1997) 411–435. doi:10.1007/bf01194788.

[21] M. D. Berrade, P. A. Scarf, C. A. Cavalcante, Conditional inspection and maintenance of a system with two interacting components, European Journal of Operational Research 268 (2) (2018) 533–544. doi:10.1016/j.ejor.2018.01.042.

[22] B. Jafary, V. Nagaraju, L. Fiondella, Impact of correlated component failure on preventive maintenance policies, IEEE Transactions on Reliability 66 (2) (2017) 575–586. doi:10.1109/TR.2017.2687426.

[23] C. D. Dao, M. J. Zuo, Selective maintenance for multistate series systems with s-dependent components, IEEE Transactions on Reliability 65 (2) (2015) 525–539. doi:10.1109/TR.2015.2494689.

[24] B. Liu, R.-H. Yeh, M. Xie, W. Kuo, Maintenance scheduling for multi-component systems with hidden failures, IEEE Transactions on reliability 66 (4) (2017) 1280–1292. doi:10.1109/TR.2017.2740562.

[25] B. Liu, Z. Xu, M. Xie, W. Kuo, A value-based preventive maintenance policy for multi-component system with continuously degrading components, Reliability Engineering & System Safety 132 (2014) 83–89. doi:10.1016/j.ress.2014.06.012.

[26] Q. Wang, F. You, F. Bai, Maintenance strategy for multi-component systems based on structure and reliability, in: 2020 11th International Conference on Prognostics and System Health Management (PHM-2020 Jinan), IEEE, 2020, pp. 309–314. doi:10.1109/PHM-Jinan48558.2020.00062.

[27] P. Múčka, International roughness index specifications around the world, Road Materials and Pavement Design 18 (4) (2017) 929–965. doi:10.1080/14680629.2016.1197144.

[28] K. F. Tee, E. Ekpiwhre, Z. Yi, Degradation modelling and life expectancy using markov chain model for carriageway, International Journal of Quality & Reliability Managementdoi:10.1108/IJQRM-06-2017-0116.

[29] V. Aryai, H. Baji, M. Mahmoodian, C.-Q. Li, Time-dependent finite element reliability assessment of cast-iron water pipes subjected to spatio-temporal correlated corrosion process, Reliability Engineering & System Safety 197 (2020) 106802. doi:10.1016/j.ress.2020.106802.

[30] C.-Q. Li, A. Firouzi, W. Yang, Prediction of pitting corrosion–induced perforation of ductile iron pipes, Journal of Engineering Mechanics 143 (8) (2017) 04017048. doi:10.1061/(asce)em.1943-7889.0001258.

[31] J. M. van Noortwijk, A survey of the application of gamma processes in maintenance, Reliability Engineering & System Safety 94 (1) (2009) 2–21. doi:10.1016/j.ress.2007.03.019.

[32] Y. Shi, Y. Xiang, M. Li, Optimal maintenance policies for multi-level preventive maintenance with complex effects, IISE Transactions 51 (9) (2019) 999–1011. doi:10.1080/24725854.2018.1532135.

[33] R. W. Bonds, L. M. Barnard, A. M. Horton, G. L. Oliver, Corrosion and corrosion control of iron pipe: 75 years of research, Journal-American Water Works Association 97 (6) (2005) 88–98. doi:10.1002/j.1551-8833.2005.tb10915.x.

[34] S. Uddin, Q. Lu, H. Nguyen, Truck impact on buried water pipes in interdependent water and road infrastructures, Sustainability 13 (20) (2021) 11288. doi:10.3390/su132011288.

[35] U.S. Department of Transportation - Federal Highway Administration, Work zone road user costs - concepts and applications (Report No. FHWA-HOP-12-005) (2011).

[36] T. M. Walski, A. Pelliccia, Economic analysis of water main breaks, Journal-American Water Works Association 74 (3) (1982) 140–147. doi:10.1002/j.1551-8833.1982.tb04874.x.

[37] American Water Works Association, American national standard for thickness design of ductile-iron pipe, ANSI/AWWA C150/A21.50-14 (2014).

[38] S. Park, R. Vega, Z. Choto, M. Grewe, Risk-based asset prioritization of water transmission/distribution pipes for the City of Tampa, Florida Water Resources Journal (2010) 22–28.

[39] Q. Lu, M. Li, M. Gunaratne, C. Xin, M. Hoque, M. Rajalingola, et al., Best practices for construction and repair of bridge approaches and departures.

[40] R. M. Clark, M. Sivaganesan, A. Selvakumar, V. Sethi, Cost models for water supply distribution systems, Journal of Water Resources Planning and Management 128 (5) (2002) 312–321. doi:10.1061/(asce)0733-9496(2002)128:5(312).

[41] Tampa Water Department, Tampa water department technical manual (Manual No. 17416) (2002).

[42] M. Hallenbeck, M. Rice, B. Smith, C. Cornell-Martinez, J. Wilkinson, Vehicle volume distributions by classification, Tech. rep. (1997).

[43] S. Amari, L. McLaughlin, H. Pham, Cost-effective condition-based maintenance using markov decision processes, in: RAMS '06. Annual Reliability and Maintainability Symposium, 2006., 2006, pp. 464–469. doi:10.1109/RAMS.2006.1677417.

[44] J. W. Kim, G. Choi, J. C. Suh, J. M. Lee, Optimal scheduling of the maintenance and improvement for water main system using markov decision process, IFAC-PapersOnLine 48 (8) (2015) 379–384, 9th IFAC Symposium on Advanced Control of Chemical Processes ADCHEM 2015. doi:10.1016/j.ifacol.2015.08.211.